FINAL REPORT

An Evaluation of Femtosecond/nanosecond Laser Induced Breakdown Spectroscopy (LIBS) for Measuring Total Particulate Emissions

SERDP Project WP-1628

MAY 2009

Dr. Mel Roquemore
Air Force Research Laboratory

Dr. Mike Brown
Innovative Scientific Solutions, Inc. (ISSI)

DoD EPA DOE SERDP
Strategic Environmental Research and Development Program

REPORT DOCUMENTATION PAGE

Form Approved
OMB No. 0704-0188

1. REPORT DATE *(DD-MM-YYYY)*	2. REPORT TYPE	3. DATES COVERED *(From - To)*
7 May 2009	Final Report	February 2008 –April 2009

An Evaluation of Femtosecond/nanosecond Laser Induced Breakdown Spectroscopy (LIBS) for Measuring Total Particulate Emissions

5a. CONTRACT NUMBER

5b. GRANT NUMBER

5c. PROGRAM ELEMENT NUMBER

6. AUTHOR(S)
Dr. W. M. Roquemore
Dr. Mike Brown, Innovative Sc
Prof. D. Hahn, University of Florida

5d. PROJECT NUMBER

5e. TASK NUMBER

5f. WORK UNIT NUMBER

7. PERFORMING ORGANIZATION NAME(S) AND ADDRESS(ES)

Air Force Research Laboratory
Propulsion Directorate
AFRL/PRTC BLDG 490
1950 Fifth Street
WPAFB OH 45433-7251

8. PERFORMING ORGANIZATION REPORT NUMBER

WP-1628

9. SPONSORING / MONITORING AGENCY NAME(S) AND ADDRESS(ES)

Strategic Environmental Research and Development Program (SERDP)
901 North Stuart Street
Arlington, Virginia 22203

10. SPONSOR/MONITOR'S ACRONYM(S)

SERDP

11. SPONSOR/MONITOR'S REPORT NUMBER(S) WO-1628

12. DISTRIBUTION / AVAILABILITY STATEMENT

Approved for Public Release Distribution Unlimited

13. SUPPLEMENTARY NOTES

14. ABSTRACT Laser Induced Breakdown Spectroscopy (LIBS) involves the dissociation of molecular species into their atomic constituents and the sequent emissions from the excited atoms. Using the LIBS signal from a sample, one can identify the atomic species and their relative concentrations. From this information and appropriate calibration curves, simple molecular species can be identified and their concentrations can be estimated. This program seeks to answer the critical question: is it feasible to develop a LIBS based technique that can be used to make a quantitative distinction between gaseous and total particulates in a multi-phase sample containing a common type atom? The approach is to investigate single and dual pulse, ns and femtosecond (fs) LIBS techniques as a way of measuring different carbon species in gaseous, aerosol, and solid phases. The program involves joint efforts between the University of Florida and the Air Force Research Laboratory (AFRL). The University of Florida investigated single, ns-LIBS and dual, ns/ns-LIBS and AFRL investigated single ns-LIBS used in conjunction with dual fs/ns-LIBS. The program was partly successful in that the ratio of the ns/ns-LIBS signal and the ns-LIBS signal could be used to determine the percentage of gaseous and total particulate carbon. This approach has promise but the sensitivity needs to be improved to become a practical technique. The fs/ns-LIBS technique was disappointing. Within the parameters studied, it could not be used to determine the percent gaseous to particulate carbon. The reason for this is not understood but is believed to be related to the plasma dynamics.

15. SUBJECT TERMS

16. SECURITY CLASSIFICATION OF:			17. LIMITATION OF ABSTRACT	18. NUMBER OF PAGES	19a. NAME OF RESPONSIBLE PERSON
a. REPORT	b. ABSTRACT	c. THIS PAGE			Dr. W. M. ROQUEMORE
U	U	U	UU	35	19b. TELEPHONE NUMBER *(include area code)* (937) 255-6813

Standard Form 298 (Rev. 8-98)
Prescribed by ANSI Std. Z39.18

Table of Contents

List of Figures

1.0 Executive Summary

This report describes the research performed on a one year limited scope program that resulted from the SERDP Statement of Need, SON 08-05. SERDP seed programs involve innovative approaches that entail high technical risk. Their purpose is to develop the data necessary to provide for risk reduction and/or a proof of concept. The following research question was raised in this Statement of Need (SON), "How can one accurately measure the total particulate emissions, including the volatile contribution?" This study investigated the feasibility of using Laser Induced Breakdown Spectroscopy (LIBS) as an approach to addressing this question.

LIBS involves the ionization or dissociation of molecular species into their atomic constituents and the subsequent emissions from electrically excited atoms. Using the LIBS signal from an unknown sample, one can identify the atomic ions, neutrals, and their relative concentrations. This information can then be used to estimate the molecular (parent) species and their concentrations in the original sample. This approach has been applied to gas, liquid, and solid samples and in some cases mixtures of molecules in different states or physical phase. However, there is a potential problem. How can one use LIBS to distinguish between species in different states of a multi phase sample? The premise of quantitative LIBS is that the sample is completely dissociated into the constituent atoms by the laser/plasma/sample interactions regardless of the molecular state or phase of the target species. This premise would discourage the use of LIBS for distinguishing between gaseous and particulate species; however, recent studies by Prof. David Hahn at the University of Florida, obtained data that suggested this premise is not correct for certain aerosol and solid particle samples. In their work, LIBS calibration curves were generated for gas, liquid aerosol, and solid particles containing carbon. It was noted that the calibration curves were all the same for different gaseous samples. However, it was demonstrated that calibration curves of LIBS signal vs carbon concentration depend, not only on the phase of the carbon sample, but on particle size and composition of the original particulates containing the carbon atoms. This raises the question: can the differences in LIBS response be used to determine the total particulates in a multi-phase sample with molecules containing a common type of atom? This is an important question because the exhaust of a gas turbine engine can have the same atomic species in multiple phases and in different types of molecules.

This program explored the question: is it feasible to develop a LIBS based technique that can distinguish between gaseous and particulate species in a way that the total particulates can be determined in a multiphase sample**?** The approach was to explore the use of nanosecond (ns, 10^{-9} s) and femtosecond (fs, 10^{-15} s) LIBS in ways that would take advantage of the difference in LIBS response to species in gaseous and particulate states. Carbon was selected for study because it is relatively straight forward to generate gaseous and particulate sample streams and because there are published results documenting the different in LIBS response for carbon in multi-phase samples. The conditions studied were not those expected in a gas turbine engine exhaust but those that were conductive to exploring new concepts for in situ measurements of total particulates. If a concept proved feasible, then it would be evaluated in more realistic environments.

The program involved a joint effort between Prof. David Hahn and the Air Force Research Laboratory (AFRL). Dr Hahn investigated a combined single- and dual-pulse ns-LIBS technique for overcoming the multi-phase problem. AFRL investigated using single ns-LIBS and dual fs/ns-LIBS

techniques. The idea of using fs-LIBS resulted from literature studies that suggest fs lasers, can dissociate a sample more efficiently than a ns laser. AFRL also investigate the question: can a fs/ns-LIBS technique provide a solution to the multi-phase sampling and partitioning problem?

This program was partly successful because of a new and innovative idea put forward by Prof. Hahn. His group demonstrated that single ns-LIBS and dual ns/ns-LIBS measurements could be used, in a unique way, to estimate the percentage of gaseous and total particulate carbon in a mixture of air, CO_2, and carbon particulates. The idea followed from the observation that the dual ns/ns-LIBS signal increased with increasing particulate carbon concentration at a different rate than the traditional single ns-LIBS signal. They obtained calibration curves that quantitatively related the dual-pulse ns/ns-LIBS and single-pulse ns-LIBS signals with the percentage of gaseous and particulate carbon. Using these calibration curves, it was demonstrated that the ratio of the dual- to single-pulse LIBS signals could be used to estimate the percentage of gaseous and total particulate carbon in a multiphase mixture. Although the sensitivity of the technique needs to be improved, Prof. Hahn's group demonstrated an approach that shows promise for distinguishing between gas and particle species. In an attempt to improve the sensitivity of Prof. Hahn's approach, AFRL investigated replacing the dual ns/ns-LIBS with fs/ns LIBS. A fs/ns-LIBS capability was established at AFRL. To demonstrate this capability, several of Prof. Hahn's critical experiments were successfully repeated using the conventional ns-LIBS technique. Single-pulse ns-LIBS and dual-pulse fs/ns LIBS were then used to obtain calibration curves for: (1) carbon dioxide, (2) oxalic acid, and (3) mixtures of air and these species. The results were similar to those of Prof. Hahn's group in that both the single and dual LIBS techniques gave a larger response to carbon from particulates than that from gases. However, the slopes of the linear calibration curves were nearly the same for the single and dual LIBS techniques. The impact was that the ratio of the fs/ns-LIBS to the ns-LIBS signals was almost independent of percent gaseous carbon. Thus, Prof. Hahn's use of single and dual LIBS to determine the percentage of gaseous and total particulate carbon did not seem to apply to the dual fs/ns-LIBS in place of the ns/ns-LIBS for the conditions studied. The cause of the difference in sensitivity of the dual ns/ns-LIBS and the fs/ns LIBS techniques is not clearly understood at this time but it is likely related to the significantly reduced interaction volume and plasma dynamics associated with the fs laser plasma.

2.0 Introduction

The EPA considers PM2.5 (particulate matter with particle sizes of 2.5 microns or less) to be the most important air pollutant because they can cause significant environmental and health problems. On 17 October 2006, the EPA issued the final amendments to the National Ambient Air Quality Standards (NAAQS) that reduce the PM2.5 24-hour standard from 65 $\mu g/m^3$ to 35 $\mu g/m^3$ (Federal Register: Oct. 17, 2006, 71, 200). This could pose problems for DoD air bases because almost all of the particles produced in gas turbine engines are PM2.5 emissions. They include solid particulates (soot) and volatile aerosols formed from condensed gases and chemi-ions. To date, attention has been directed primarily at the carbonaceous particulate matter. However most of the particulate emissions in aircraft exhaust are in the form of condensed volatile aerosols. These particulates can grow via continuing condensation and agglomeration. They consist mostly of acids, such as H_2SO_4/H_2O, HNO_3/H_2O and $H_2O/H_2SO_4/HNO_3$, as well as neat H_2O. These aerosols can have a significant impact on both the local and global environment by providing surface areas for heterogeneous chemistry and sinks for already present atmospheric condensable gases. These effects are not understood nor have they been adequately characterized. This was recognized in the SERDP SON 08-05 in which the following research question was raised, "How can one accurately measure the total particulate emissions, including the volatile contribution?"

3.0 Background

A literature search was performed to identify promising diagnostic techniques for distinguishing the phase of solid and volatile aerosol particles in gas turbine engine exhaust. Laser-Induced Breakdown Spectroscopy (LIBS) was identified as a promising technique because it has the potential of measuring: total mass, composition, number density, and particle size of both solid and aerosol particles. There are numerous ns-LIBS studies involving the detection of solid particles and aerosols. Some of the papers involved in sulfur particles are reviewed in this section. There are relatively few studies involving using ns-LIBS to obtain quantitative analysis of a species in different phases (gaseous, liquid, and solid) in the same sample. The difficulties of multiphase ns-LIBS measurement that are most relevant to this study are illustrated in the research performed by Prof. David Hahn at the University of Florida. Important aspects of his research are also discussed in this section. In recent years fs-LIBS has evolved as an important diagnostic tool but it has not been extensively investigated as a quantitative method of analysis. Some background on fs-LIBS is also provided in this section.

3.1 Conventional ns-LIBS

Radzlemski *et al* [1983] were the first to determine the atomic species composition of aerosols using LIBS. However, it has been only in the last 10 years that LIBS has been used to obtain total mass, composition, and size distributions of particles [Hahn, 1997; Hahn, 1998]. Since this revelation, LIBS has been used in numerous solid and aerosol particle studies. Some background on LIBS and the results from several relevant LIBS studies are presented in this section to illustrate its potential for making both solid and aerosol particulate measurements. Most LIBS studies use ns pulse lasers. Thus, conventional LIBS is sometimes referred to as ns-LIBS to distinguish it from fs-LIBS performed with fs pulse lasers.

LIBS is an atomic emission spectroscopy technique that makes use of transient laser-induced micro-plasmas that serves as both the sample volume and excitation source [Hahn, 2000; Lee, 2004; Song, 1997]. All molecules and particles less than 10 μm are dissociated in the micro-plasma. The optical emission consists of a plasma continuum and atomic emission lines corresponding to the elemental composition of the sample. The wavelength of the individual emission lines identifies the elemental composition and their relative intensity indicates the concentration of the individual species. The emitting atoms and ions are excited through collisions with hot electrons, ions, and other atoms. The plasma exists for a few μs to ms. While the plasma kinetics are quite complex, knowledge of the details of the dynamics is generally not needed to effectively use LIBS. The sensitivity and quantifiable nature of LIBS measurements are made through systematic calibration of individual LIBS instruments. Attributes of the technique include *in situ* operation, multi-elemental analysis, relatively simple data reduction, high sensitivity, and space- and time-resolved real-time measurements. For most species, detection limits lie in the few ppm and below. LIBS has been used for analysis on solid surfaces, soil samples, gas samples, ice particles [Arp 2004], and aerosols. Measurements are readily made in harsh ambient environments such as reacting flows. The spatial distribution of H and O atoms in hydrogen/air diffusion flames has been measured and favorably compared with simulations [Itoh 2001]. Trace metals have been detected at ppm levels in industrial boilers and furnaces [Blevins, 2003]. More recently, LIBS was demonstrated as a means for engine health monitoring via the detection of seeded Mg [Baldwin, 2006]. In addition to the seeded Mg, Fe from actual engine wear was also detected in this proof-of-concept study.

A recent study has demonstrated that LIBS can be used to determine the composition and total mass of sulfuric acid aerosols produced in controlled homogeneous nucleation experiments [Nunez, 2000]. Even though the measurements were made in a controlled environment, this is an important demonstration because most of the particulate emissions from gas turbine engines are in the form of condensed volatile material with the dominant aerosol species being H_2SO_4/H_2O [Karcher, 1998-b; Penner, 1999]. Aviation fuels contain sulfur that is largely emitted in the nascent exhaust as SO_2. Through a series of chemical kinetic steps, the gaseous SO_2 becomes H_2SO_4/H_2O (sulfuric acid) forming the most abundant volatile aerosols. Nunez [2000] generated the aerosol droplets at room temperature by passing bulk liquid sulfuric acid of varying concentrations through a nebulizer into a bath of either air or argon.

A sample LIBS spectrum of three S emission lines obtained by Nunez *et al* [2000] is presented in Figure 3.1. Such spectra were recorded over a range of known sulfuric acid concentrations permitting an absolute concentration calibration. The results of the calibration run are shown in Figure 3.2. From the calibration work, the researchers determined a sulfur detection limit of 0.38 ppm of sulfuric acid aerosol with their experimental setup. The authors noted that this *does not* represent the absolute lower limit of detection. Their detection limit was dictated by hardware limitations and not the LIBS technique itself. In Figure 3.2 the S ns-LIBS signal is correlated with both sulfur concentration by weight and the sulfuric acid mass density.

Aerosol size distributions can also be determined from LIBS signals [Hahn, 2000]. Figure 3.3 shows the size distribution of Ca-based particles determined by ns-LIBS measurements. The results are presented as a histogram and compared with the particle size distribution as determined by a commercial particle sizer using a light scattering methodology. The agreement between the two techniques is quite good. Individual particle diameters were determined from the calibrated linear relationship between mass

concentration and LIBS signal, the measured plasma volume (sample volume), and the known density of individual Ca particles.

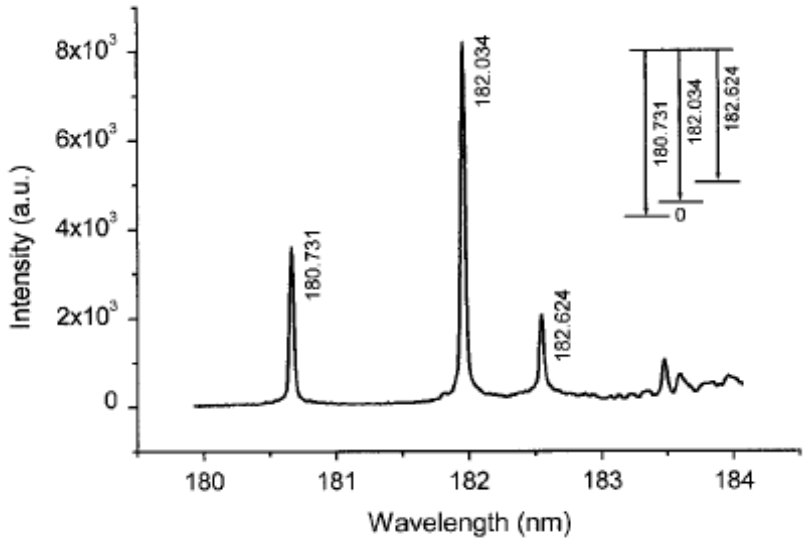

Figure 3.1. ns-LIBS spectrum of sulfuric acid aerosols in the vicinity of the three sulfur emission lines used for concentration measurements. (Taken from Nunez 2000.)

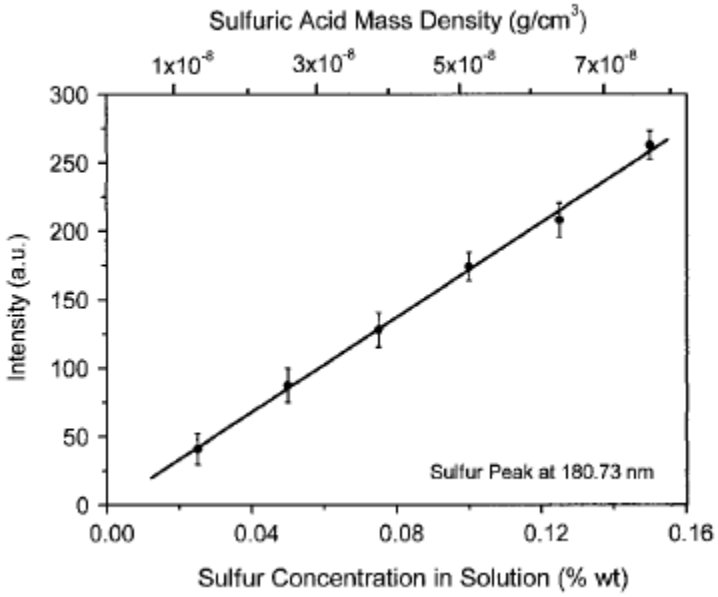

Figure 3.2. Calibration of ns-LIBS signal for sulfur emission taken from sulfuric acid aerosols. The ns-LIBS signal scales linearly with the sulfur concentration in the parent liquid (by weight %) and with the sulfuric acid mass density in the probe volume. (Taken from Nunez 2000.)

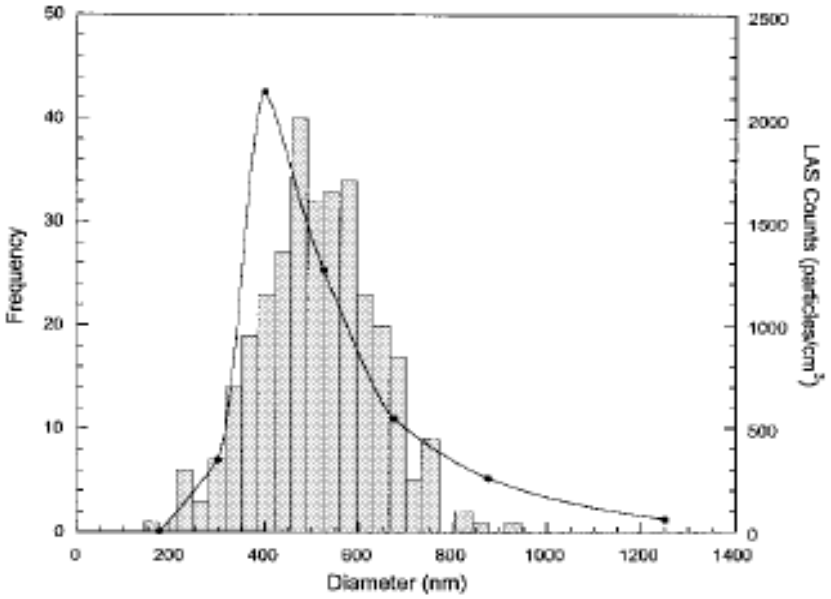

Figure 3.3. Particle size histogram determined from LIBS signals recorded in a stream of Ca-based particles with co-flow of nitrogen at 1 atm. The bars indicate the LIBS-based particle size measurements. The solid line indicates the size results obtained using a commercial particle sizer. (Taken from Hahn 2000.)

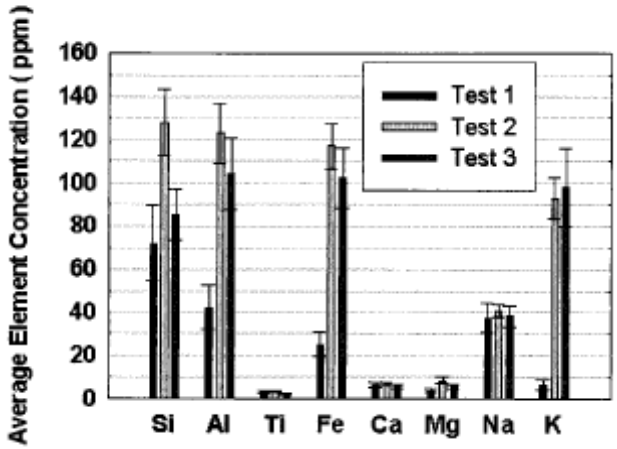

Figure 3.4. The elemental metal composition of the exhaust stream of a biomass coal burner for three different fuels obtained from ns-LIBS measurements. The spectral features of 8 different metals were monitored simultaneously. (Taken from Blevins 2003.)

It is clear from the above that ns-LIBS can be used to determine the mass concentration and individual particle size of particulates and aerosols. Composition of multi-component flows can be determined as well. This is illustrated by the work of [Blevins, 2003] who simultaneously detected 8 trace metals in the exhaust of a biomass coal burner at 1170 K (See Figure 3.4). Thus, there is significant research that

illustrates LIBS can be used to obtain particle size distributions and identify the particle composition. What has not been clearly demonstrated is whether LIBS can be used to distinguish between an analyte in gas, liquid aerosol and solid particles in the same sample like would occur in the exhaust plume of a gas turbine engine.

A critical issue is whether fs/ns-LIBS can distinguish between gases, liquid aerosols, and solid particles in simple and complex environments. Recent results obtained by Hohreiter suggests this is a real problem. They investigated the LIBS spectra of carbon in gas and solid phases. The gas phase carbon was in the form of CO_2, CO, and CH_4. The solid carbon was in the form of 30-nm polystyrene (C_8H_8) and oxalic acid $(COOH)_2$ particles. As noted in Figure 3.5, the intensities of the carbon spectra lines are different for the different forms of carbon. Figure 3.6 shows how the carbon spectral intensity changes with carbon concentration. Note that all the LIBS intensities, for carbon in the gas phase, are on the same curve. However, the curve for the LIBS C intensities, for the higher density oxalic acid (1.9 g/cm^3) particles, has a larger slope than that for the polystyrene particles with a density of 1.0 g/cm^3.

The issue raised by Hohreiter and Hahn of whether LIBS can always distinguish between gas, liquid, and solid phase of an analyte is the main focus of this paper. Their results were obtained using ns-LIBS. An important issue to address is whether the same problem would occur using fs-LIBS, which is a relatively new field. A short background of fs-LIBS is given in the next section.

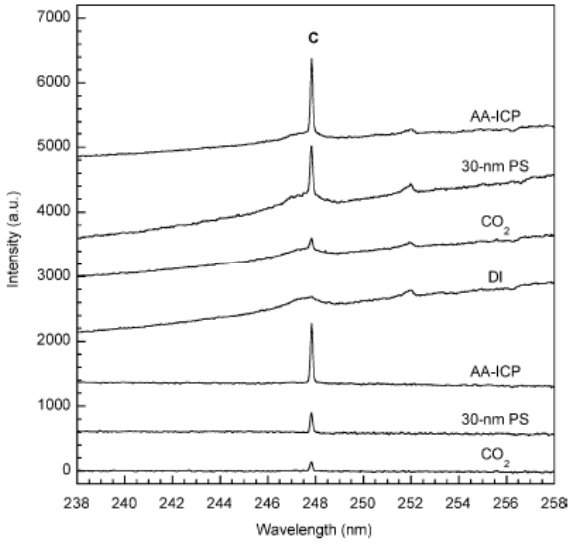

Figure 3.5. LIBS spectra for different sources of carbon. All the spectra have the same scale and have been shifted vertically for clarity. (From Hohreiter 2005.)

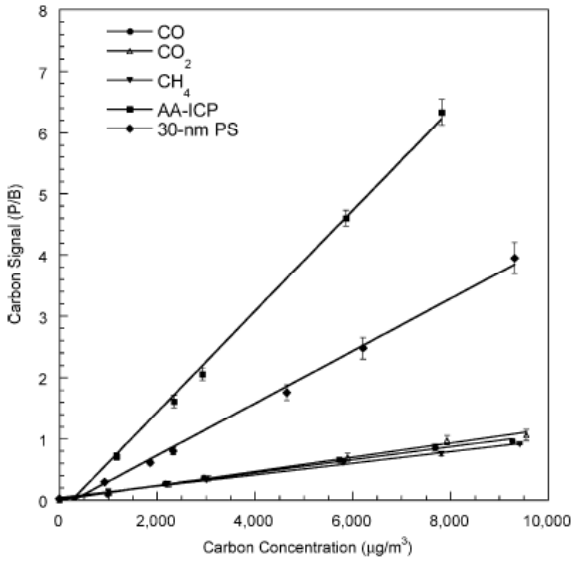

Figure 3.6. Calibration curves based on C atomic emission line for 5 carbon analyte sources. (From Hohreiter 2005.)

3.2 Femtosecond fs-LIBS

Historically, LIBS became a popular diagnostic technique because of the availability of reliable nanosecond pulsed lasers in the 1970s. For example, excimer and Nd:YAG ns pulse lasers produce a plasma by achieving focused intensities of $>10^9$ W/cm^{2,} which are above the breakdown potential of most samples. This results in electron temperatures of about 15,000 K. Today, a new generation of LIBS is evolving because of breakthroughs in laser technology. The invention of chirped-pulse amplification and reliable femtosecond lasers has resulted in the availability of tabletop, fs pulse lasers, with focused intensities greater than 10^{19} W/cm^2. Such ultra-short-pulse, ultra-intense focused intensities, referred to as extreme light [Mourou, 2002], interact with matter in completely new ways that can be advantageous to LIBS. For example, the plasma created with extreme light results from field ionization of both the outer and inner electrons in a sample. This results in plasmas with a higher density of electrons and higher collision rates than that produced by a ns laser. This is important because the higher collision rate of the electrons with the atomic species can result in more intense, richer emission spectra. The net result of this is that fs-LIBS has the potential of having higher signal to noise ratios and higher accuracy than ns LIBS. This has been demonstrated in some recent fs-LIBS studies [see for example Margetic 2000]. Ppm detection limits for minor species in Al alloys have been demonstrated [Le Drogoff 2001].

4.0 Results and Discussion

This program explored the question: is it feasible to develop a LIBS based technique that can be used to obtain the percentage of particulates in a gaseous/particulate multi-phase mixture? The approach was to explore the use of nanosecond (ns, 10^{-9} s) and femtosecond (fs, 10^{-15} s) LIBS in ways that would take advantage of the different in LIBS response to species in gaseous and particulate states as observed by [Hohreiter and Hahn, 2005]. The approach involved a joint effort between Prof. David Hahn and the Air Force Research Laboratory (AFRL). Dr Hahn investigated different ns-LIBS techniques that might be used to overcome the multi-phase problems. The literature suggests that a femtosecond (fs, 10^{-15} s) pulse laser decomposes a sample into constitute atoms more efficiently than a ns laser. AFRL investigated using fs-LIBS techniques along with a combined fs/ns-LIBS techniques as a means of solving the multi-phase problem. The results of these studies are presented in this section.

Carbon was selected as the species to study because it is relatively straight forward to generate gaseous and particulate sample streams and because there are published results documenting the different in LIBS response for carbon in multi-phase samples. The conditions studied were not those expected in a gas turbine engine exhaust but those that were conductive to exploring new concepts for in situ measurements of total particulates. If a concept proved feasible, then it would be evaluated in more realistic environments..

4.1 Experimental Methods for University of Florida Activities

Dual and single-pulse LIBS measurements were made using various mixtures of gaseous and particulate carbon. Single-pulse LIBS measurements were recorded using a 1064-nm Nd:YAG laser (denoted Laser 1) with 300 mJ/pulse energy operating at 5 Hz repetition rate. All analyte samples flowed through a standard six-way vacuum cross at atmospheric pressure, which functioned as the LIBS sample chamber. A gaseous co-flow of 44 lpm of purified air was used for all experiments. The air was passed through an activated alumina dryer, a course particle filter, an additional desiccant dryer, and finally a HEPA filter cartridge prior to entering the sample chamber. All flow rates were controlled with digital mass flow controllers. The aerosolized carbon particles were made by nebulizing a solution of oxalic acid

at a rate of about 0.15 ml/min using a gas flow of 5 lpm through a pneumatic type nebulizer (Hudson model #1724). The carbon solutions were prepared by diluting ICP-grade analytical standards of 10,000 μg C/ml [SPEX CertiPrep] to the desired concentration using ultrapurified deionized water. The solution concentrations were adjusted to provide a range from about 3 to 20 μg C/liter of gas through the LIBS sample chamber. Based on previous TEM measurements using the current configuration, the average aerosol particle size following droplet desolvation (i.e. solid analyte phase) is expected to be less than about 100 nm, while agglomerate formation is considered insignificant. For gaseous-phase carbon, carbon was introduced to the sample chamber as a specified flow of carbon dioxide using an additional mass flow controller. Experimental conditions were adjusted such that the percentage of solid-carbon to gaseous-carbon could be varied from 10% gas-phase carbon and 90% particulate phase carbon (as elemental carbon by mass) to 90% gas-phase carbon and 10% particulate phase carbon. Specific conditions tested were 10/90 (gas/solid percentages), 25/75, 50/50, 75/25 and 90/10 gas/solid percentages. For each gas/solid mixture, the overall carbon concentration was then increased while the percentage was held constant.

For all experiments, the plasma was created in the center of the sample chamber using a 50-mm diameter, 75-mm focal length lens. The plasma emission was collected on axis with the incident laser beam (Laser 1) using a pierced mirror and 75-mm focal length condensing lens. The plasma emission was then fiber-coupled to a 0.275-m spectrometer (2400 groove/mm grating, 0.15-nm resolution). Spectral data were recorded using an intensified CCD detector array. For all experiments, the ICCD was synchronized to the laser Q-switch, and the detector delay and integration times were set to 8 μs and 5 μs, respectively. For the dual-pulse configuration, an additional laser-induced plasma was created using a similar 1064-nm, 300 mJ/pulse laser (denoted as Laser 2) oriented orthogonal to the first laser such that the laser-induced plasma was created at the exact same focal volume as created for Laser 1. For all dual-pulse experiments, Laser 2 was fired 1 μs prior to Laser 1, which was estimated to be an optimal separation based on extensive previous dual-pulse measurements [Windom, 2006]. For each carbon concentration and gas/solid mixture, each measurement was recorded using six individual 1000-shot averages spread over multiple days for both the single-pulse LIBS (Laser 1 only), and the dual-pulse LIBS (Laser 2 1 μs prior to Laser 1) configurations. All data were processed using the 247.9-nm carbon I atomic emission integrated over the full-width, and normalized to the adjacent continuum plasma emission (Bremsstrahlung emission), to yield the final Peak-to-Base ratio (P/B) as the analyte signal.

Figures 4.1.1 and 4.1.2 show representative single- and dual-pulse LIBS spectra that correspond to 90% gas-phase carbon and 10% solid-phase carbon (90/10). Also, 10% gas-phase carbon and 90% solid-phase carbon (10/90) are also shown. Several features are noted in these spectra, which were consistent for all of the experiments performed. First, for all cases the absolute intensity of the dual-pulse configuration was reduced with respect to the corresponding single-pulse condition. This was observed for all gas/solid carbon mixtures. This effect is consistent with previous experiments [Windom, 2006], and corresponds to the fact that the first laser-induced plasma (Laser 2) creates a rarefied condition into which the second laser (Laser 1) is fired. The rarefaction created by the first laser reduces the resulting plasma emission from the plasma created by the second laser. For analysis of *solids* via dual-pulse LIBs, the rarefaction created above the solid by the first laser helps to "clear" the target from the cover gas, thereby creating better coupling from the second pulse into the target, resulting in more analyte emission from the solid target, and less continuum emission from the ambient gas. However, with pure gaseous breakdown as in the current study, the rarefaction serves to significantly lower the plasma continuum

emission because the continuum arises primarily from the gas-phase species, which have been subsequently rarefied by the first plasma event. The second observation is that the 247.9-nm carbon emission signal was observed to increase when increasing the percentage of carbon as particulate solid carbon (i.e. decreasing the gas/solid carbon mixture fraction). This trend was observed for both solid and dual-pulse LIBS configurations. To quantify the data, the P/B ratio was calculated for all total carbon concentrations and for all gas/solid carbon mixtures.

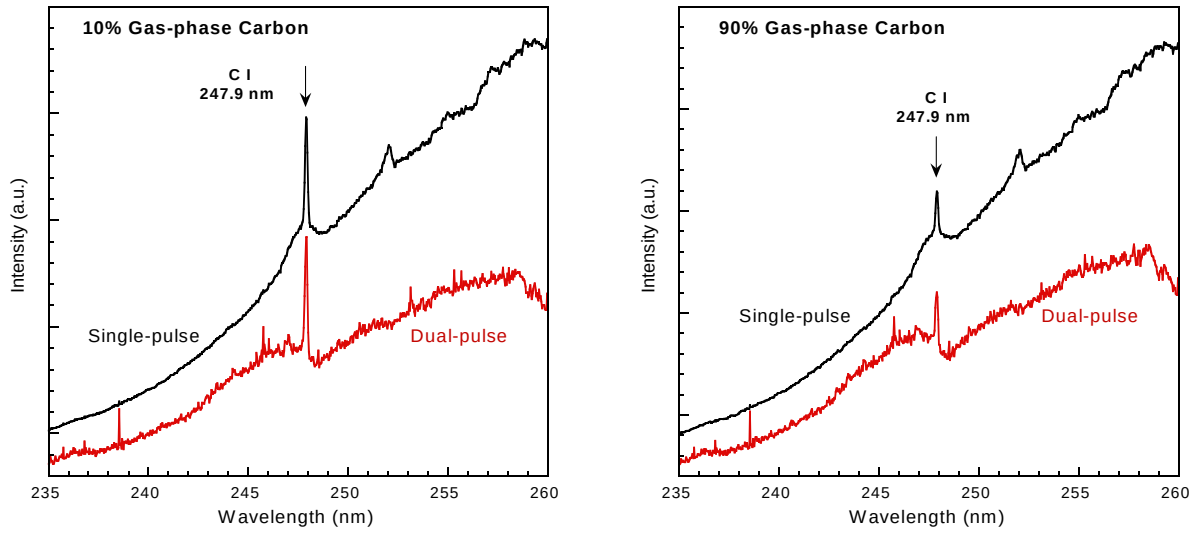

Figure 4.1.1 and 4.1.2. 1000-shot average LIBS spectra for 10% gas-phase carbon (left) and for 90% gas-phase carbon (right) for both single-pulse and dual-pulse LIBS.

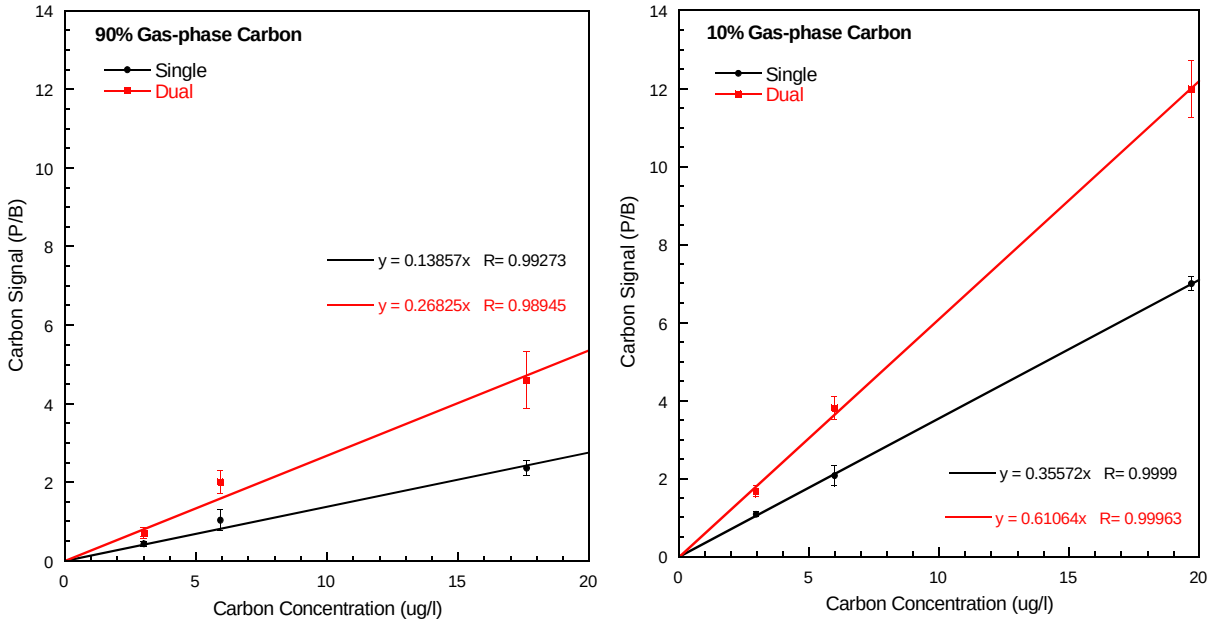

Figure 4.1.3 and 4.1.4. LIBS calibration curves for 90% gas-phase carbon (left) and for 10% gas-phase carbon (right) for both single-pulse and dual-pulse LIBS configurations.

By varying the overall carbon content while maintaining a constant gas/solid carbon mixture fraction, calibration curves were prepared for each specific mixture using both the dual-pulse and single-pulse configurations. Two such calibration plots are presented in Figures 4.1.3 and 4.1.4 for the 10% gas-phase and 90% gas-phase carbon conditions, respectively. All calibration curves yielded excellent linearity and a nearly zero y-intercept value, although a slight trend of reduced correlation coefficients was observed with increasing gas/solid content ratio. It is noted that a zero y-intercept value is required for a robust analytical calibration curve.

The above calibration curves reveal an increased slope with increasing solid carbon content (i.e. decreasing gas/solid mixture fractions), which is in agreement with the above discussions regarding Figures 4.1.1 and 4.1.2. *Clearly the carbon signal is enhanced with increasing percentage of solid-phase analyte.* While it was not so apparent in the raw spectra, it is also observed that the carbon P/B signal is in fact *enhanced* with the dual-pulse configuration as compared to the single-pulse configuration for both gas-phase mixtures presented above, as evidenced by the increase in slope when comparing the dual-pulse calibration plot to the single-pulse calibration plot for a given gas/solid mixture. The above calibration plots were also prepared for the 25/75, 50/50, and 75/25 gas/solid carbon mixtures, yielding results consistent with the above trends. To examine the overall behavior of carbon response over the entire experimental matrix, the resulting calibration curve slopes are presented in Figure 4.1.5 as a function of gas/solid carbon mixture fractions for both the single and dual-pulse configurations. As observed in

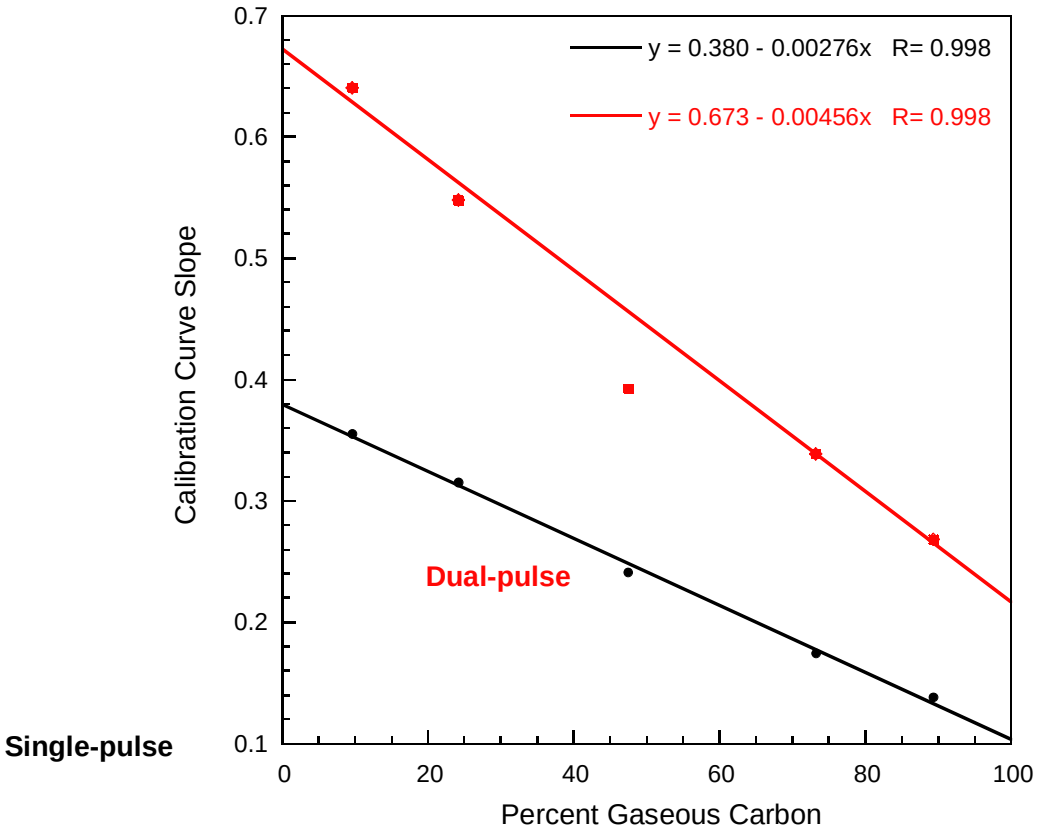

Figure 4.1.5. Individual slopes of the LIBS calibration curves as a function of the percent gaseous carbon ranging from 10% to 90%, for both the single and dual-pulse cases.

Figure 4.1.5 for any given percentage of gaseous carbon, the slope of the dual-pulse LIBS calibration curve always exceeds the single-pulse LIBS calibration curve slope. For a given configuration (i.e. single or dual-pulse), the calibration curve slope is always observed to increase as the percentage of gaseous carbon is decreased (i.e. increasing solid carbon content). Furthermore, the trend line fit to the calibration curves slopes of the single-pulse LIBS experiments is very linear over the range of gaseous/solid mixtures explored. The corresponding curve fit to the dual-pulse experiments is also rather linear in nature; although the 50/50 data point (50% gas phase/50% solid phase) does sit somewhat below the linear trend line. This behavior was consistently observed, and the offset is well outside the expected error bars.

The results presented in Figure 4.1.5 suggest an interesting observation, namely, that the ratio of the single-pulse to dual-pulse response (as reflected by the calibration curve results) reveals a steady trend as the percentage of gaseous carbon varies over the range of 10% to 90%. The concept was further evaluated by using the two trend lines to calculate the ratio of the dual-pulse to single-pulse response as a function of percentage of gaseous carbon. A plot of this dual/single carbon response is presented in Figure 4.1.6 over the range of experimental conditions. In addition, the actual calibration curve slopes are included for the 10/90, 25/75, 75/25 and 90/10 gas/solid cases. *Most importantly, the ratio of the dual/single pulse response does display a monotonic response over the range from 10% to 90% gaseous carbon*. While the

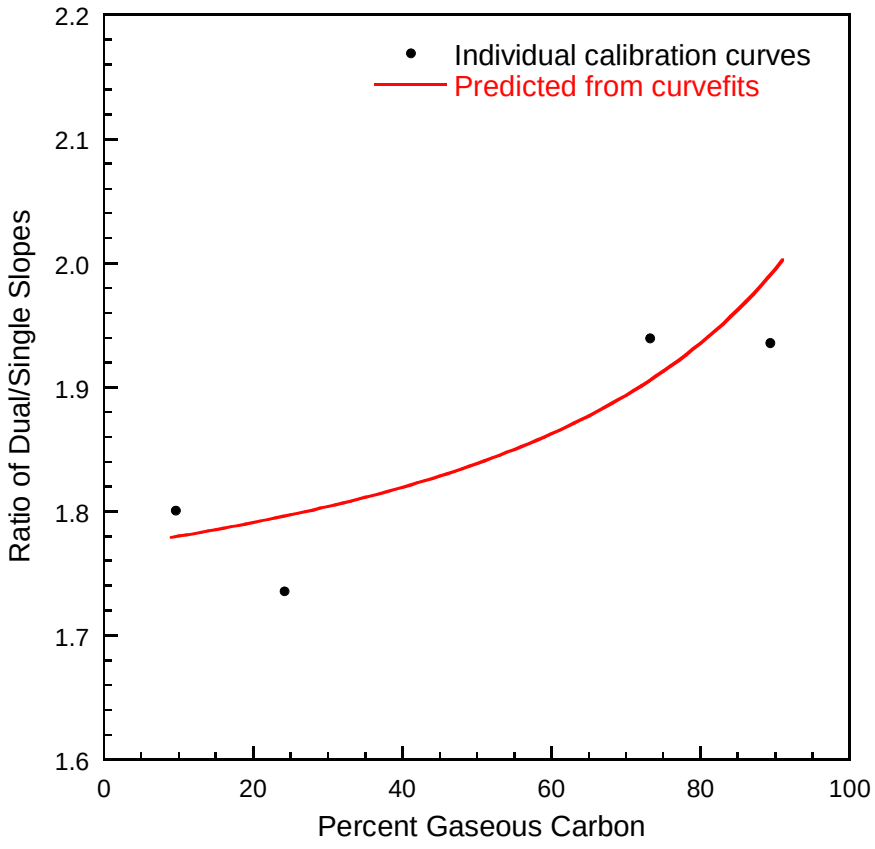

Figure 4.1.6. Ratio of the dual-pulse to single-pulse calibration curve response as predicted from the trend lines of Figure 4.1.5 and as measured from the individual calibration curves, as a function of the percent gaseous carbon ranging from 10% to 90%.

individual calibration curve points show some variation, they also follow this general trend. It is rather remarkable that given the considerable variation in LIBS response of the carbon line when comparing single or dual-pulse configurations, or when comparing the various percentages of gaseous carbon, the ratio of dual/single pulse LIBS response is remarkably consistent, and furthermore, displays a monotonic response over the mixture fraction range examined in the current study.

Figure 4.1.6 illustrates that the ratio of dual- and single-pulse LIBS signals can be used to estimate the percentage of gaseous and total particles in a multi-phase sample. This technique utilized the result that gaseous, liquid aerosol, and solid particulates result in a different calibration curves for dual and single pulse LIBS. As observed in this and previous studies, there exist significant differences in the LIBS response of solid-phase analyte as compared to gaseous-phase analyte [Hohreiter, 2005], with the former being more pronounced. In addition, the dual-pulse configuration provides an enhanced analyte response (as measured by the P/B ratio) although the absolute signal levels are reduced. Such an effect is consistent with the rarefaction produced by the first laser-induced plasma, and the fact that particulatephase species are somewhat resistant to the rarefaction relative to gas-phase species. When these two observations are combined, the use of the dual/single pulse LIBS response is shown to be a potentially useful method for measuring the total particulate and gaseous species containing carbon. However additional studies are needed to determine the full potential of this technique.

4.2 fs/ns LIBS at Propulsion Directorate Air Force Research Laboratory

The research at AFRL differed from that at the University of Florida in that a combined fs/ns LIBS system was set-up so that independent measurements could be made using either fs or ns LIBS. The fs and ns lasers could also be electronically coupled so that one could be used as a pre-pulse and the other the main pulse. This system was used to reproduce the importance results of Hohreiter and Hahn, 2005. Once their results had been reproduced, the combined system was used to investigate the feasibility of using the dual LIBS technique described in Section 4.1 to distinguish between the gas and solid carbon analyte but using the fs laser as the pre-pulse and the YAG as the main LIBS pulse. This research is described in this section.

4.2.1 Experimental Set-up

A schematic of the optical setup for the work reported here is shown in Figure 4.2.1. Two laser systems were employed in the measurements enabling measurements in both a one-pulse and two-pulse format. The single-pulse measurements were made using a 10-Hz frequency-doubled Nd:YAG laser delivering 6-ns pulses at 532 nm with pulse energies ranging from 290 – 680 mJ. The double-pulse measurements combined the output of the Nd:YAG laser with the output of a Ti:sapphire regenerative amplifier delivering 45-fs pulses at 1 kHz with a central wavelength of 800 nm. The pulse energy was varied from 400 – 750 μJ. The laser pulses from the two systems were synched to each other electronically using a master/slave arrangement. The Ti:sapphire laser operated as a master clock controlled by its intrinsic electronics. A clock pulse from these electronics was input to a custom-built divide-by box the output of which delivered 10-Hz pulses to a delay generator. Two output pulses from

the delay generator triggered the flashlamp and Q-switch of the Nd:YAG laser. The same delay generator also triggered the controller for the ICCD camera used to acquire the LIBS signals.

Beams from both lasers were combined using a dichroic mirror and directed through a pierced mirror to a common focusing lens that placed the focus of both beams at the center of the LIBS chamber. The dichroic mirror transmitted the 800-nm light and reflected the 532-nm light. Most of the single-pulse gas-phase carbon data was acquired using a 150-mm focusing lens placed exterior to the chamber. The single-pulse solid-phase carbon data along with all of the double-pulse data was collected using a 40-mm focusing lens placed inside one arm of the LIBS chamber. The arrival time of the laser pulses in the sample chamber was monitored using a photodiode placed near the chamber.

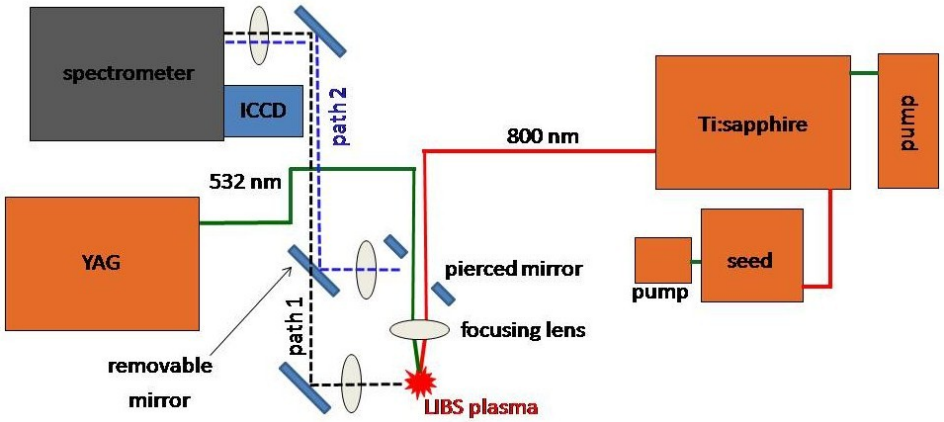

Figure 4.2.1. Schematic of the dual laser system LIBS setup used for this study. As indicated by "path 1" and "path 2" labels, two LIBS signal collection geometries were employed. For path 1 the LIBS signal was collected at 90-degrees to the incident laser beams and for path 2 the signal was collected in the backward direction using a pierced mirror. For clarity, only the mirrors directing the collected LIBS emission are shown. See text for details.

The pierced mirror permitted the collection of the LIBS signal in the backward emission direction. (See path 2 in Figure 4.2.1.) This geometry enables collection of the LIBS signal from nearly the entire plasma volume reducing sensitivity to shot-to-shot changes in the axial location of the LIBS plasma breakdown location. For this collection path, the focusing lens doubles as the collection lens. The optical setup also included signal collection at 90-degrees with respect to the propagation axis of the lasers through the chamber. (See path 1 in Figure 4.2.1.) All of the double-pulse data was collected using this. Switching between collection paths was achieved simply by removing or replacing the "removable mirror" shown in Figure 4.2.1. The collection lenses for both signal collection paths collimate the LIBS signal which is then directed by mirrors to a common lens (350-mm) that focuses the light into the ¾-m single-grating spectrometer. The exit slit of the spectrometer was removed and replaced with an intensified charge-coupled device (ICCD) camera that served as the detector. The ICCD was operated in imaging mode yielding a 2-D signal map with wavelength along one axis and spatial location on the orthogonal axis. The recorded spatial dimension is normal to the propagation axis of the laser pulse for both collection axes.

The target chamber (see Figure 4.2.2) was constructed following the design of Hahn [2001] and suspended between two laser tables in the laboratory room. The incident laser beams were focused at the

center of a six-way cross. The four equatorial arms were fitted with quartz windows to permit straight-thru passage of the laser beams as well as signal collection and visualization of the laser sparks. The top of the cross was open to an active exhaust hood that drew the sample flow effluent out of the room. The bottom of the cross was connected to the analyte/solute delivery system. Solid-phase carbon samples in the form of aerosols were delivered into the target area using a commercial medical-grade nebulizer made by Hudson. Carbon in the form of dilute oxalic acid [atomic absorption grade supplied by Spex Certiprep] was loaded into the nebulizer by unscrewing the reservoir from its top. A 5 l/min supply of dry nitrogen (99.999% pure) was fed into the nebulizer from a computer-controlled mass-flow-controller. At this gas flow rate 0.15 ml/min of fluid was introduced into the drying tube. The resultant mass loading of carbon in the sample chamber was altered by repeated dilution of the oxalic acid with de-ionized water. Solid carbon in the form of polystyrene spheres was also introduced into the chamber by placing samples of the spheres (also diluted with de-ionized water) into an atomizer that was plumbed in place of the nebulizer. To prevent sample-to-sample contamination, individual nebulizers were used for each sample type and for each carbon concentration. For gas-phase carbon measurements, no material was placed inside the nebulizer reservoir. The nebulizer simply acted as a pass-through for carbon-containing gas delivered through the 5 l/min mass flow controller. Most of these measurements were made using a research-grade bottle of 100 ppm CO_2 in N_2. The output of nebulizer was directed through a hole cut in the center of the sintered metal disk.

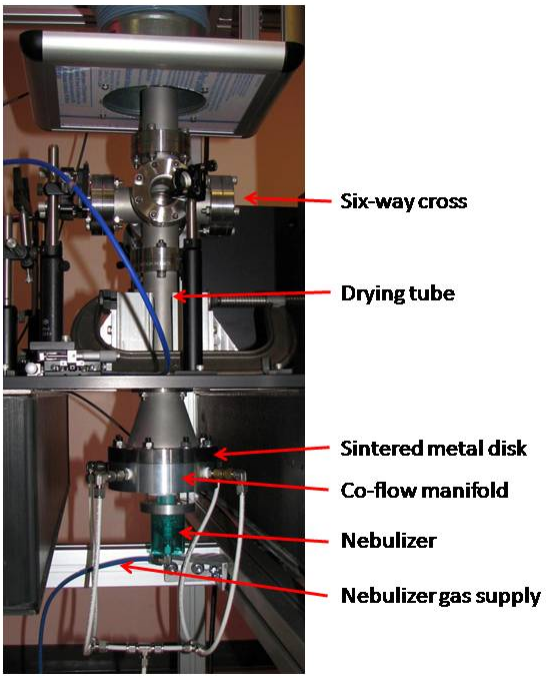

Figure 4.2.2. LIBS chamber used for all data collection presented here. Design based on work by Dr. Hahn and co-workers.

Further dilution and delivery of the nebulizer effluent was accomplished using a co-flow of N_2 (99.999% pure) metered by a 50 l/min mass flow controller. The co-flow passed through the sintered metal disk ensuring laminar flow in the drying tube. The co-flow rate was varied to maintain a total gas flow rate into the chamber of 40 – 45 l/min. The combination of this total flow rate and the length of the

drying tube insured that dry aerosol particles of carbon entered the laser focus area with mean diameters of less than 100 nm as determined by Hahn's group using the original test chamber based on the same design [Hohreiter, 2005]. We note that all measurements regardless of analyte source were made at atmospheric pressure. Similarly all measurements were made under flowing conditions.

4.2.2 LIBS signal acquisition and processing

A LIBS signal consists of one or more atomic lines from the emitting analyte superimposed on the broadband plasma emission. The broadband emission consists largely of bremsstrahlung from the free electrons as they cool along with some recombination emission. If the LIBS signal is acquired over a large wavelength range (many tens of nm or more) atomic (and molecular) features associated with the environmental gas (e.g. air) are typically present as well. For most of the work reported here, carbon served as the analyte. In Figure 4.2.3 the strong 248-nm emission line from the neutral carbon atom is shown sitting on top of the broadband plasma. The broadband emission is present in all LIBS measurements at varying degrees of intensity. Consequently, LIBS signals are typically reported as peak-to-base ratios (P/B). As shown in the Figure 4.2.3, the peak is given by the integrated area of the analyte emission line above the broadband emission (baseline or base). For the data reported here, we adopt the definition used by Hahn's research group for the base [Hohreiter, 2005]. Numerically, the base is given by the value of the baseline at line center. The peak-to-base ratios shown in the figures that follow represent averages over multiple laser shots, typically 600-1000 depending on the strength of the signal.

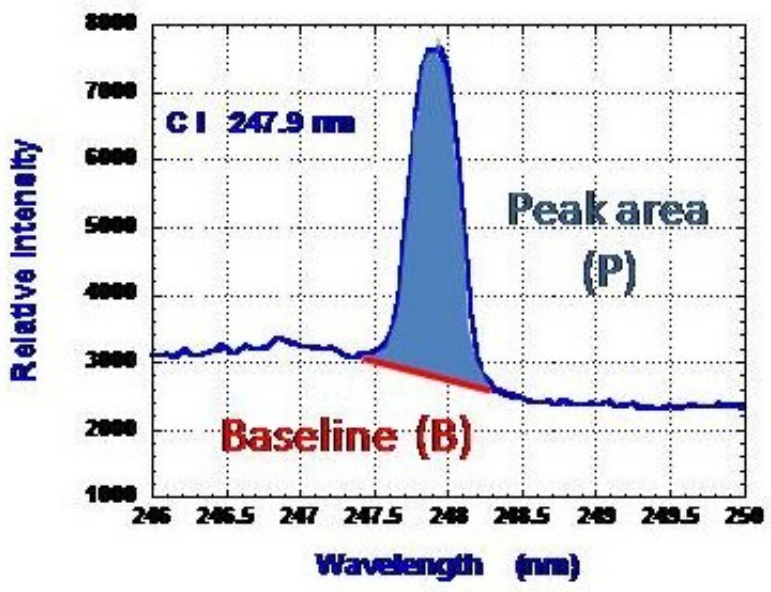

Figure 4.2.3. Graphical representation of Peak and Baseline. The peak-to-base ratio (P/B) is defined as the ratio of the peak area to the midpoint value (value at line center) of the baseline.

For each experimental condition of carbon source and solute, three types of ICCD images were acquired: (1) a background image acquired with the laser blocked, (2) a "blank" image of just the analyte, and (3) a signal images of the analyte/solute source at varying conditions of the test parameter. The test parameters included laser pulse energy, detection gate delay and gate width, solute phase, and solute

concentration. For each experimental condition, a background and blank image were recorded at both the beginning and end of the parametric run. All four of these images were recorded using the same number of laser shots as the parametric signal images. The pre- and post-run background and blank images were compared to ensure that no systematic signal collection changes had occurred during the parametric run. No sign of such systematic drift was ever seen indicating the robustness of the setup. This observation is consistent with the findings of Dr. Hahn and his group.

The acquired ICCD images were processed using custom routines written in Matlab. The background image was subtracted from each blank and signal image to remove electronic noise. The background-corrected blank and signal images were then processed to produce corresponding spectra. This was accomplished by summing the individual rows in the images along the spatial dimension. Care was taken to exclude the rows which lay outside the region of strong emission. This has an indirect effect of improving signal-to-noise ratios. The signal spectra were processed with the corresponding blank spectra. The baseline of the signal spectra were subtracted from the desired atomic line emission using the blank spectra (scaled as need be). The baseline-corrected signal spectra were integrated across the atomic emission feature to yield a numerical value for the peak. The line center value of the blank spectrum was used for the base and the peak-to-base ratio was then calculated. This procedure was repeated for each signal image acquired in each parametric study. The Matlab routines were constructed to either process a single signal image or batch process a collection of related images. All of the data presented in the following figures was processed in this way and is presented in the form of peak-to-base ratio (P/B) versus the test parameter.

4.2.3 ns-LIBS with gas-phase carbon

Gas-phase carbon LIBS measurements excited by ns pulses provided a good means to verify common results between the work done at WPAFB and the Univ. of Fla. Figure 4.2.4 shows the peak-to-base ratios for gas-phase carbon LIBS signals from CO_2/N_2 mixtures as a function of carbon mass loading in units of micrograms per cubic meter. Three sets of measurements are shown: two made at WPAFB using pulse energies of 350 and 680 mJ/pulse, and the third at the Univ. of Fla. using a pulse energy of 290 mJ.

As seen, the signal strength has at most a weak dependence on the pulse energy. This is consistent with the current wisdom of the LIBS community. More importantly, the slopes of the P/B ratios versus mass loading are nearly identical between our two collaborative working groups (see Figure 4.2.5). The agreement between the two sets of measurements ensures that the hardware setups in both laboratories yields similar measurement environments and that the signal processing routines yield common numerical results.

Work at the Univ. of Fla. has shown that all gas-phase sources of carbon yield a common LIBS signal (P/B) dependence on mass loading in a common solute (air in this instance). Hence, we can comfortably assume that our results shown in Figure 4.2.4 and Figure 4.2.5 are transferable to any gas-phase carbon source such as methane, carbon monoxide, or the vapor of any heavy hydrocarbon fuel.

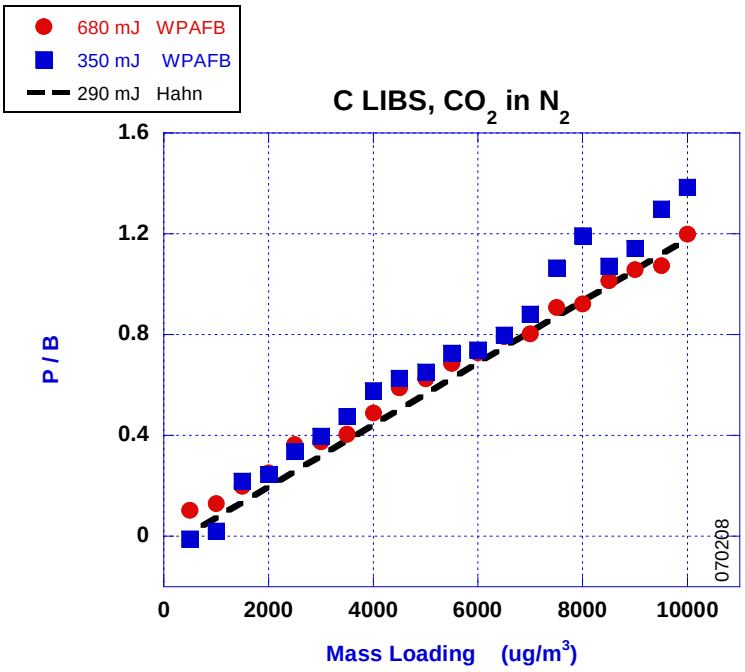

Figure 4.2.4. Measured peak-to-base ratios for two pulse energies compared with results from (Hohreiter and Hahn, 2005) (Univ. of Fla.). (Backward light collection.) Error bars equal to size of markers.

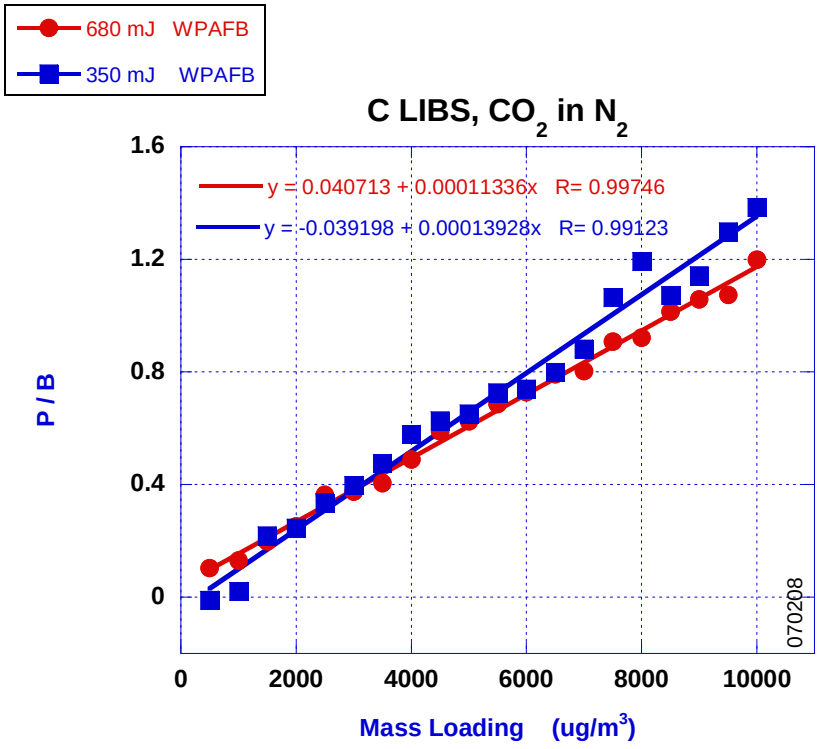

Figure 4.2.5. Linear fits to the data of Figure 4.2.4. Slope for corresponding work by Hahn et al = $1.16e^{-4}$.

Two of the key experimental parameters for LIBS measurements are the detector delay and gate width. The delay is with respect to the arrival of the excitation laser pulse in the sample chamber (Refer to Figure 4.2.13 ignoring the first laser pulse). The temporal characteristics of the plasma emission and atomic analyte emission typically differ as the plasma evolves. The initially hot electrons cool largely via bremsstrahlung and later, after having lost much of their initial kinetic energy, they collisionally excite the desired atomic emission. While individual electrons may lose their energy at differing rates with a well-defined statistical loss rate for the ensemble, generally speaking, most lose much of their energy early in the plasma evolution. As a consequence, the background plasma emission tends to decay faster than the atomic emission of interest. We examined this for a fixed mass loading of carbon from a CO_2/N_2 mixture by measuring the peak-to-base ratios and the peak ratios as a function of gate delay for three settings of the gate width (3, 6 and 12 μs). Results of these measurements are shown in Figure 4.2.6. Consistent with published results, the peak-to-base ratios increase with increasing delay until a maximum value is reached and the ratios decrease rapidly for greater delays. Over the same range of gate delays the peak signal (wavelength-integrated emission) decreases and consequently the signal-to-noise ratio decreases. Selection of detector gate delay is then a matter of compromise between peak-to-base and signal-to-noise ratios. For the work presented here, the gate delay was typically set to 10 or 12 μs.

The dependence of the observed LIBS signal on gate width is much weaker than that on the gate delay. As seen in Figure 4.2.6 and Figure 4.2.7, increasing the gate width by a factor of 4 only increases the measured signal by a factor of ~20% or less. Most of the data reported here was recorded with a gate width of 10-12 μs.

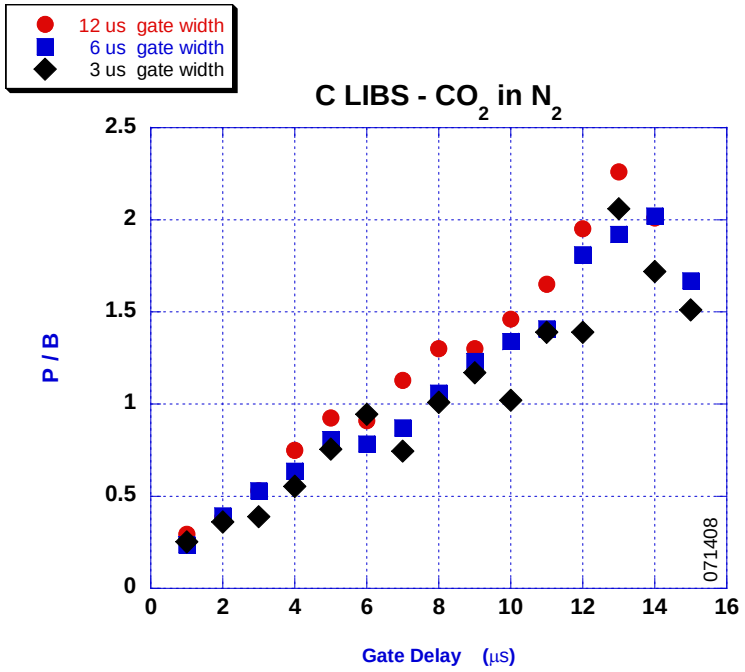

Figure 4.2.6. Measured peak-to-base ratios as a function of gate delay for three values of the gate width.

The LIBS plasma volume is best characterized as an ellipsoid with the long axis lying on the propagation direction of the incident laser pulse. Regardless of the signal collection direction with respect to laser propagation axis, the entrance slit of the spectrometer acted as a limiting aperture. Figure 4.2.9 indicates the relative relationship between the LIBS plasma volume and the sub-volume passed through the spectrometer. The plasma volume is characterized by gradients in electron temperature and density. Both are greatest near the center of the ellipsoid and decrease radially and longitudinally with distance from the center. Therefore, changes in signal collection direction that in turn change the affective aperture lead to a sampling of somewhat different plasma conditions for the same laser spark.

The data shown in Figure 4.2.4, Figure 4.2.5, Figure 4.2.6, and Figure 4.2.8 was recorded using the backward collection geometry (path 2 of Figure 4.2.1). In this geometry, the slit passes all emission along the beam propagation axis simply eliminating the side lobes of the emission region (c in Figure 4.2.9). In this way both cold and hot regions of the plasma contribute to the recorded LIBS signal. With the 90-degree geometry the slit preferentially selects the hot region of the plasma (d in Figure 4.2.9) and this impacts the observed signal. Figure 4.2.10 shows the peak-to-base ratios for gas-phase carbon versus mass loading taken with the 90-degree collection geometry. Comparing with equivalent ratios recorded in the backward geometry (Figure 4.2.5) we see that peak-to-base ratios are of nearly equal value. The difference lies in the slope which is 13% less for the 90-degree collection data set. While this is not a large difference it is statistically significant and emphasizes the fact that LIBS calibration procedures need to be executed using the same geometry planned for the measurements of unknown analyte concentration.

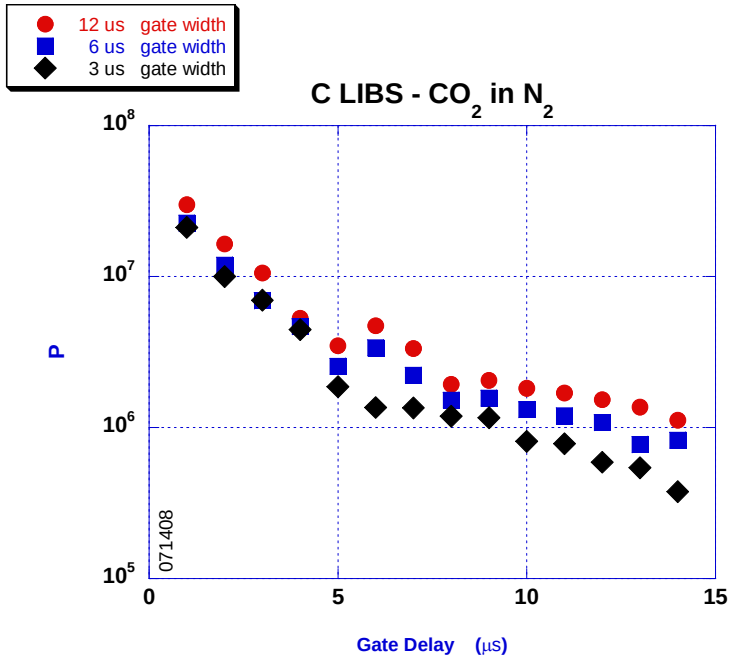

Figure 4.2.7. Measured peak carbon signal as a function of gate delay and gate width. Compare with Figure 4.2.6.

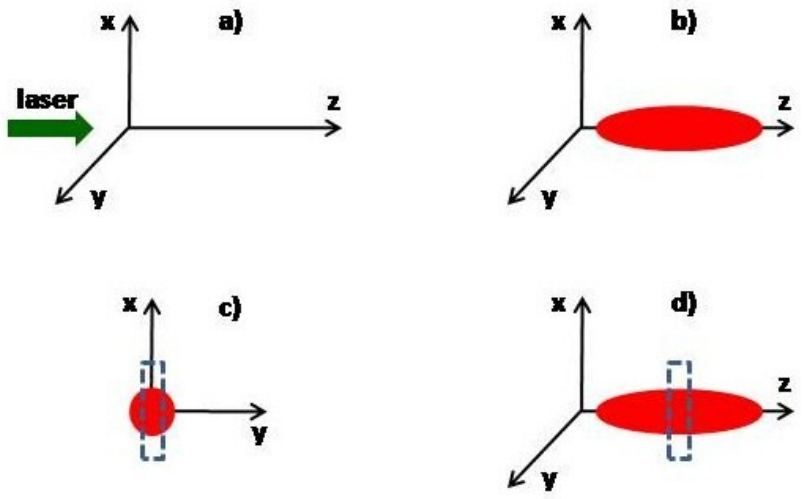

Figure 4.2.8. Schematic indicating the aperturing of the LIBS plasma volume by the entrance slit of the spectrometer. (Slit indicated by the gray rectangular box.) The LIBS plasma appears as an ellipsoid with the long axis collinear with the propagation axis of the laser, b). c) and d) indicate the portion of the ellipsoid that passes through the spectrometer slit for backward, c), and 90-degree, d), light collection. (See Figure 4.2.1 for light collection geometry.)

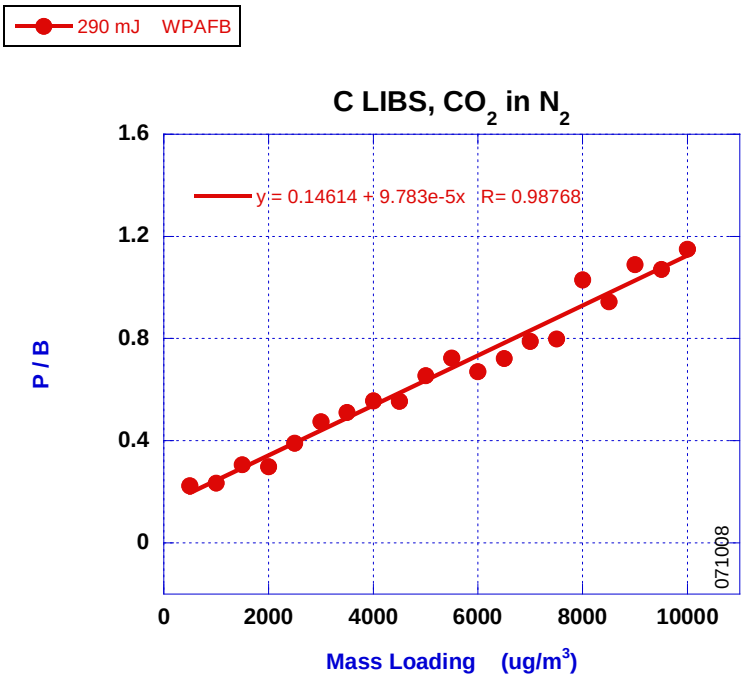

Figure 4.2.9. Measured peak-to-base ratios versus mass loading for 90-degree light collection (path 1 in Figure 4.2.1). Compare with Figure 4.2.4. Ns-LIBS on solid-phase carbon (aerosol particles)

4.2.4 ns-LIBS with solid –phase carbon (aerosol particles)

LIBS measurements on solid-phase carbon particles were executed by loading dilute samples of oxalic acid in the nebulizer. The high-purity stock sample of oxalic acid (1000 mg of C per ml) was obtained from Spex Certi-prep and varying mass loadings were obtained through dilution with de-ionized water. Using the flow rates noted in section 4.2.1, carbon in the form of small aerosol particles was delivered into the sample volume in a flowing manner. Based upon previous studies by Hahn and coworkers at the Univ. of Fla., the aerosol particles are known to have diameters of less than 200 nm. Peak-to-base ratios for our work and the work at the Univ. of Fla. are shown in Figure 4.2.10. The slopes of the signals are roughly seven times that of the gas-phase carbon signal (see Figure 4.2.5) over the same range of mass loadings. This confirms the observation by Hahn and coworkers and Chang and coworkers that LIBS signals of the same analyte are dependent upon the physical phase of the analyte. This difference is related to the details of how the energy in the incident laser pulse is transported into the sample volume, and the hydrodynamic response of the plasma. For gas-phase samples the excitation of individual analyte atoms occurs via direct electron impact excitation or electronic energy cascade following recombination of an electron and an analyte ion. For aerosol particles, excitation energy must first be transported macroscopically into the interior of the aerosol via thermal transport.

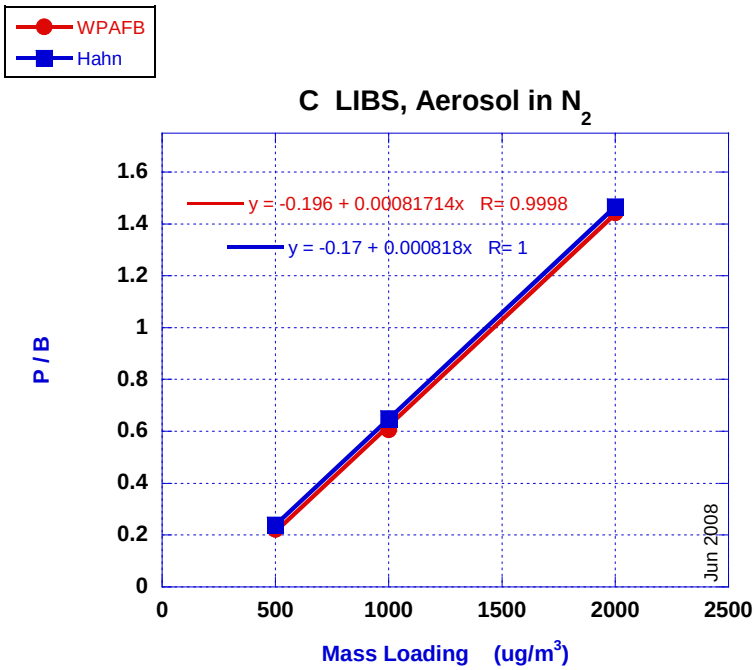

Figure 4.2.10. Comparison of peak-to-base ratios for carbon in aerosol form (oxalic acid) versus mass loading for the data collected with the setup at WPAFB and at the Univ. of Florida (Hahn). Backward light collection.

It is well-known that when energy is impulsively deposited at a single geometric point, the subsequent gas dynamic response generates radial gradients in the pressure, temperature and density of the surrounding medium as a blast wave emanates from the point of energy deposition [Zeldovich, 1966].

While the LIBS spark is spatially distributed (on the scale of tens of microns) it is very likely that such a blast wave will sweep material radially outward from the initial spark volume. The lighter gas-phase material will be more easily swept out than the solid-phase material which will offer inertial resistance to such movement. Consequently, on the spatial scale of the initial LIBS spark, the mass density of solid-phase analyte will be closer to that of the pre-spark state than that of the gas-phase analyte. Both the details of energy transport and hydrodynamic response could play a role in the observed difference of LIBS signals for gas and solid-phase analytes over similar ranges of mass loading. An important part of this research effort is finding ways to exploit this phase-dependent aspect of the LIBS signal, since the aircraft exhaust environment is characterized by individual analytes in multiple phases.

4.2.5 ns-LIBS with solid-phase carbon (polystyrene spheres)

LIBS measurements were made on solid-phase carbon in the form of polystyrene spheres. For this work, the nebulizer was replaced with a TSI atomizer. Monodispersed samples of known carbon concentration were purchased from Duke Scientific. The atomizer was loaded with fixed concentrations of carbon on a mass basis. In order to characterize the sample within the LIBS spark volume, a differential mobility analyzer (DMA) was connected to an extractive sampling tube the end of which was placed within the flowing sample stream about one cm away from the spark location. The DMA was

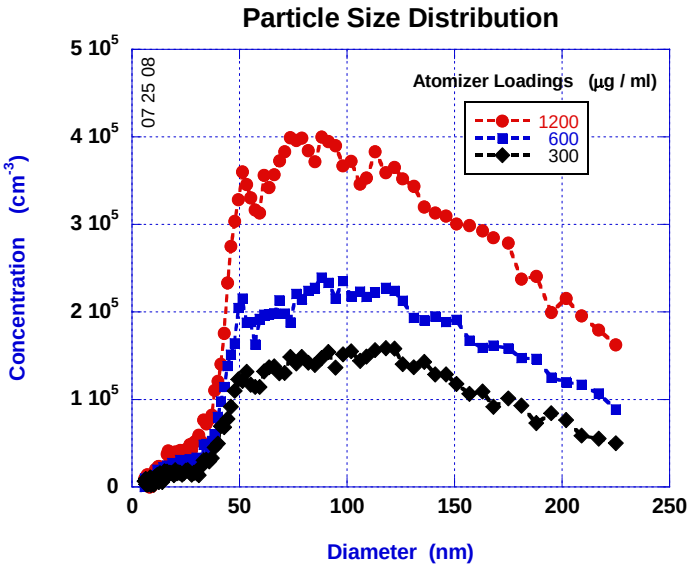

Figure 4.2.11 Particle size distribution determined by a differential mobility analyzer for the Duke Scientific 50-nm polystyrene spheres. Agglomeration above an effective diameter of 225 nm is unknown as these sizes lie outside the operating range of the analyzer. Compare with Figure 4.2.12.

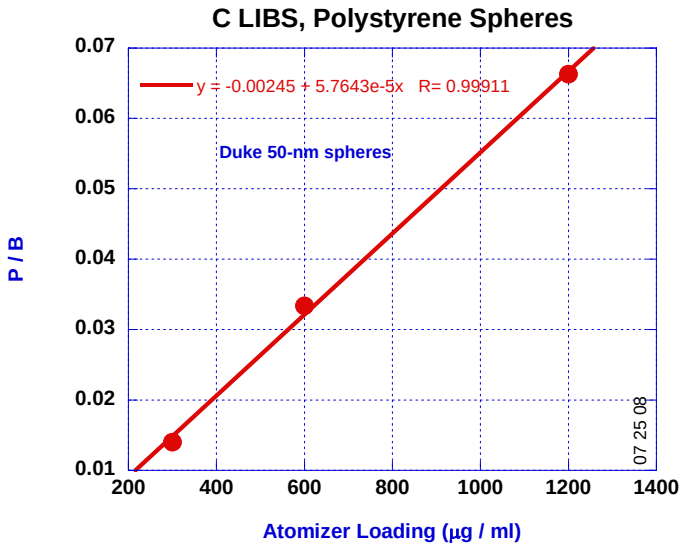

Figure 4.2.12. Peak-to-base ratios for the LIBS signals associated with the particle size distributions shown in Figure 4.2.11.

paired with a particle counter and the combination provided a particle size distribution in the form of concentration (number of polystyrene spheres per cubic centimeter) per mean particle diameter. The particle size distribution for the 50-nm polystyrene spheres is shown in Figure 4.2.11 for three atomizer mass loadings. Clearly the mono-dispersed sample is heavily agglomerated. The reason for this is that the sample did not contain a surfactant (which contained carbon) for keeping the particles dispersed. We attempted to disperse the polystyrene spheres by mixing for many hours but were not successful. Polystyrene is a dielectric and small spheres can easily acquire enough charge to electrostatically cling to one another. In principle it is possible to determine the carbon mass loading within the LIBS spark using the particle size distribution. However, the DMA configuration prevented detection of agglomerated spheres with effective diameters greater than 225 nm. The size-limited particle size distribution is insufficient to confidently recover the mass loading in the LIBS target volume. However, it is meaningful to report the LIBS peak-to-base ratios as a function of atomizer mass loading. This is done in Figure 4.2.12 for the sample reported in Figure 4.2.11. Note that the P/B ratios are a linear function of atomizer loading. This suggests that it is possible to make quantitative LIBS measurements on agglomerated analyte particles.

4.2.6 fs-ns dual-LIBS with gas and solid-phase carbon (CO_2 and aerosol particles)

As evidenced by the work done by our collaborators at the Univ. of Fla., dual-pulse LIBS based on two ns pulses delayed with respect to each other yields a means to quantitatively determine the relative amounts of gas-phase and solid-phase carbon in a mixed sample over a range of total mass loadings. We examined another dual-pulse approach using a combination of fs and ns pulses. While the fs pulses deliver much less energy than the ns pulses (0.5 mJ vs 300 mJ), their peak field intensity is orders of magnitude higher and they efficiently ionize the target sample via the tunneling mechanism. The lower pulse energy also produces plasma that is much shorter lived – tens of ns as compared to tens of µs.

However, in principle, a LIBS detection scheme that begins with a fs pulse that is closely followed by a ns pulse (see Figure 4.2.13) may yield complimentary phase discrimination. The leading fs pulse can potentially influence the LIBS signal by either rarifying the sample volume hydrodynamically or by producing a pre-ionized sample volume that more readily absorbs more energy from the second ns pulse than if the fs pulse were not present.

The LIBS spark produced by the fs laser pulse is significantly smaller than that produced by the ns laser pulse. Like the ns-pulse-excited spark, the fs-pulse-excited spark is elliptical in shape with the long axis collinear with the laser propagation direction. To ensure that any preconditioning produced by the fs pulse was taken advantage of fully, the two incident laser beams were combined (see Figure 4.2.1) and focused with a common optic (singlet) along a common propagation axis. A singlet lens was used for this purpose. To compensate for the different focal lengths of the lens at 532 and 800 nm, two-lens telescopes were placed in both laser beam paths to alter the divergence of the two beams as they entered the singlet. (Recall that a singlet will focus "blue" light faster than "red" light.) Images of the two laser sparks appear in Figure 4.2.14. The two spark images have been displaced vertically for clarity. They do in fact lie on a common axis. The ns-pulse-excited spark is not entirely symmetric along the propagation axis. The peak plasma emission tends to appear closer to the leading edge of the spark than the trailing edge. With this in mind, the beam telescopes were adjusted to get the fs spark to lie as close as possible to the location for peak emission within the ns spark. The distance between the center of the fs spark and the peak emission point of the ns spark was minimized to 750 μm. Any further reduction of this spatial separation will require the use of a custom-designed air-spaced doublet or triplet. Since breakdown of the surrounding medium does not necessarily happen right at the waist of the focused ns beam, (Breakdown can initiate

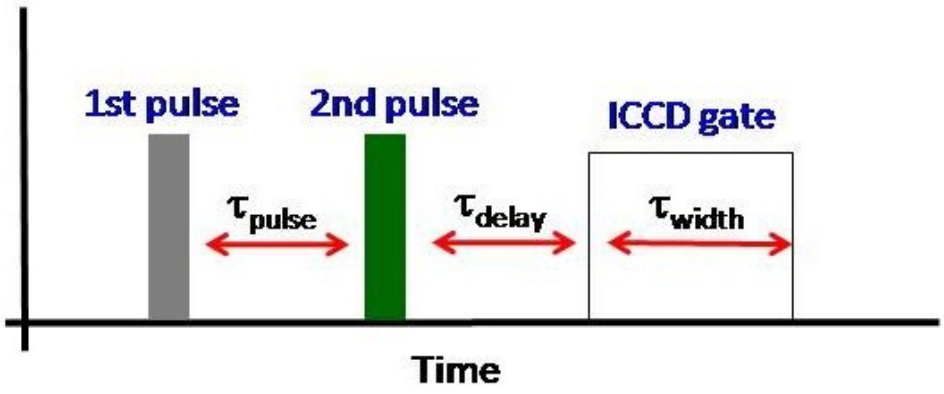

Figure 4.2.13. Timeline for the dual-pulse LIBS experiments. For the work done at the Univ. of Fla., both pulses were delivered from a ns laser. For the work done at WPAFB, the first pulse was delivered from an fs laser and the second from a ns laser.

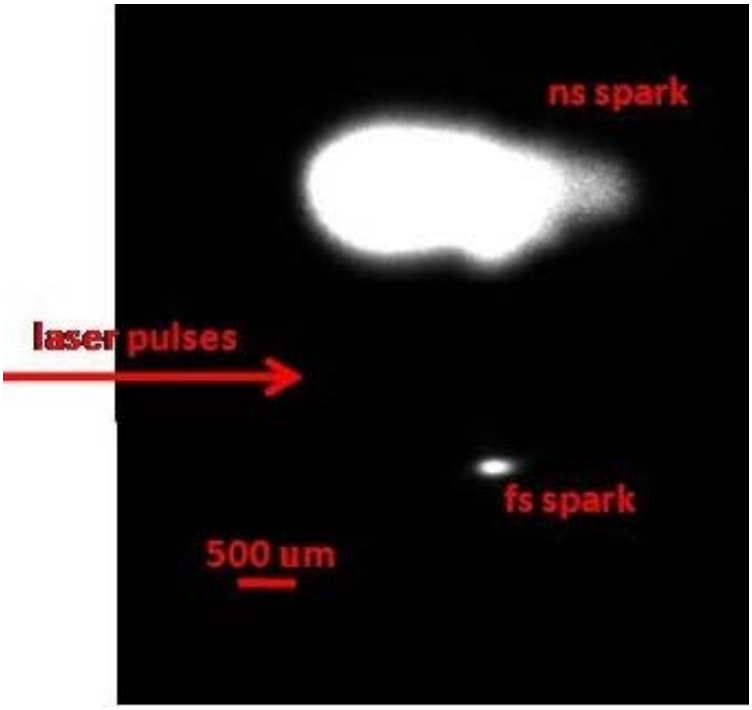

Figure 4.2.14. Images of fs and ns laser sparks collected at 90-degrees. The spark images have been displaced vertically for clarity. The fs spark appears 750 μm behind the location of the peak ns spark plasma emission.

upstream of the waist position), care must be taken in this design to permit some independent user adjustment of the two spark locations.

It is well known that focused fs pulses with intensity characteristics of the laser used in this work (>10^{14} W/cm^2) yield forward and backward emission due to self-phase modulation and stimulated Raman processes. Such emission may offer its own unique diagnostic utility, particularly for even larger focused intensities. For the work reported here, we chose to collect the LIBS signal at 90-degrees to ensure that we only studied signals attributable to the dual-pulse setup. The collection optics were arranged such that the spatial location of the fs spark and the back end of the ns spark were imaged into the spectrometer. The LIBS signal from this spatial location will necessarily exhibit the largest dual-pulse effects but is unlikely to be the region of greatest emission. In this sense the data was collected using an optical compromise given the restrictions of the hardware available to the program.

With the two laser sparks overlapped as noted, measurements were taken of the peak-to-base ratios for gas-phase carbon (CO_2 in N_2) as a function of delay between the two pulses for two values of the fs pulse energy – 500 and 750 μJ. The detector gate delay and gate width were both held fixed at 10 μs. The gate delay with respect to the ns pulse is indicated in Figure 4.2.13. For both pulse energies the difference between the dual and single-pulse LIBS signals peaked for a pulse delay of 500 ns. This delay setting was then used for all of the P/B measurements as a function of mass loading and phase mixture fraction. Based on these measurements we cannot say with certainty whether the influence of the fs pulse on the LIBS signal is due to ratification or pre-ionization. Such discernment would require a much more extensive fundamental study.

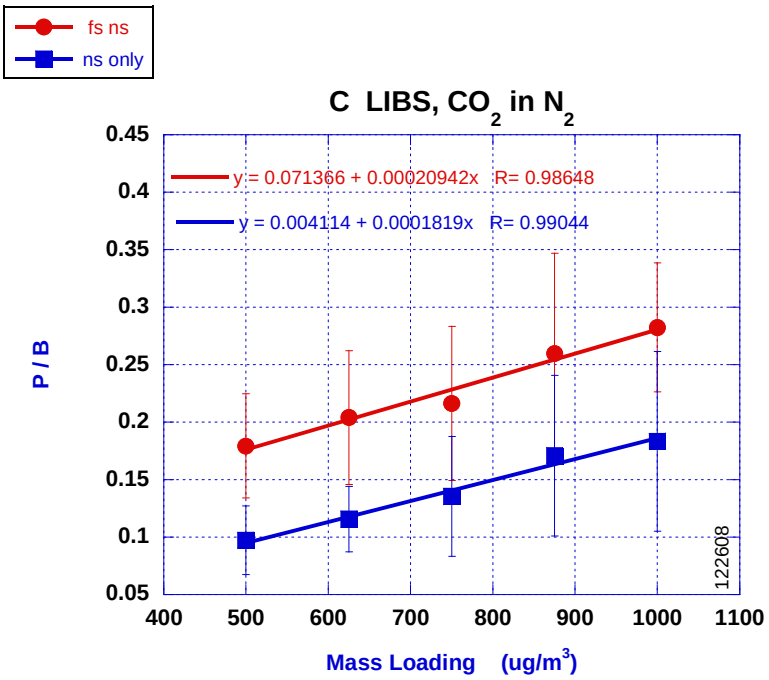

Figure 4.2.15. Peak-to-base ratios for fs-ns and ns-only excitation of carbon in gaseous phase as a function of the mass loading in the chamber.

The peak-to-base ratios for the dual pulse (fs-ns) and single pulse (ns-only) measurements on gas-phase and solid-phase (aerosol) carbon are shown in Figures 4.2.15 and 4.2.16, respectively. Similar to the results found by our collaborators at the Univ. of Fla. using two ns pulses, the dual-pulse LIBS signal is larger than the single-pulse signal. As anticipated, both modes exhibit a linear relationship between the LIBS signal and the mass loading. Also, as seen in the dual-pulse approach with two ns pulses, the signal increases faster for the solid-phase sample as a function of mass loading. We note that the dual-pulse work involving two ns pulses was performed at higher carbon mass loadings. For example, a mass loading of 10 µg/L on the ns-ns data corresponds to a mass loading of 10,000 µg/m^3 on Figure 4.2.15 and Figure 4.2.16. However, given the linearity of LIBS signals over very large ranges of mass loadings as reported in the literature, it is very unlikely that this difference affects the conclusions reached in this study.

Following the measurements on samples of single-phase carbon, dual and single-pulse LIBS measurements were made on mixtures of gas and solid-phase carbon at a fixed total mass loading. Results for a total mass loading of 5000 µg/m^3 are shown in Figure 4.2.17. The data are plotted as a function of the percentage of the total mass in gas phase. Just as for the study using the two ns pulses, the LIBS signals decrease with increasing percentage of gas-phase carbon. Likewise, the dual-pulse signal (fs-ns) is larger than the single-pulse (ns-only) signal. The difference lies in the relative slopes between the fs-ns case and the ns-only case. The two calibration curves are very parallel to each other. This is highlighted by examining the ratio of the signals in the two cases. As seen in Figure 4.2.18, within the measurement uncertainties, the ratio of the two signals for the two modes (dual-pulse and single-pulse) is constant as a function of percent gaseous carbon. Hence, at least for the stated measurement conditions it would be

difficult to determine the relative amounts of gas and solid-phase carbon using an fs-ns dual-pulse LIBS measurement.

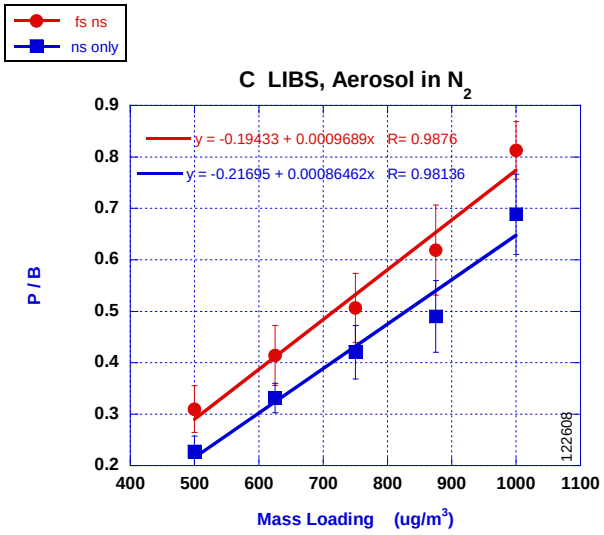

Figure 4.2.16. Peak-to-base ratios for fs-ns and ns-only excitation of carbon in aerosol phase as a function of the mass loading in the chamber.

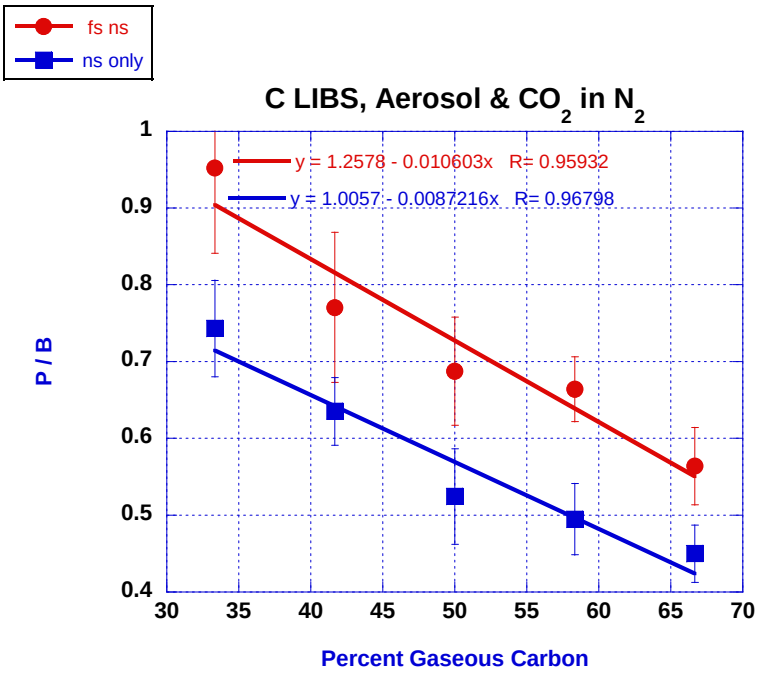

Figure 4.2.17. Peak-to-base ratios for fs-ns and ns-only excitation of carbon in CO_2/aerosol mixtures as a function of the percent of gaseous carbon present. Downward slopes are indicative of stronger LIBS signals from the aerosol phase. For each mixture, the total mass loading of all carbon present was held to 5000 $\mu g/m^3$.

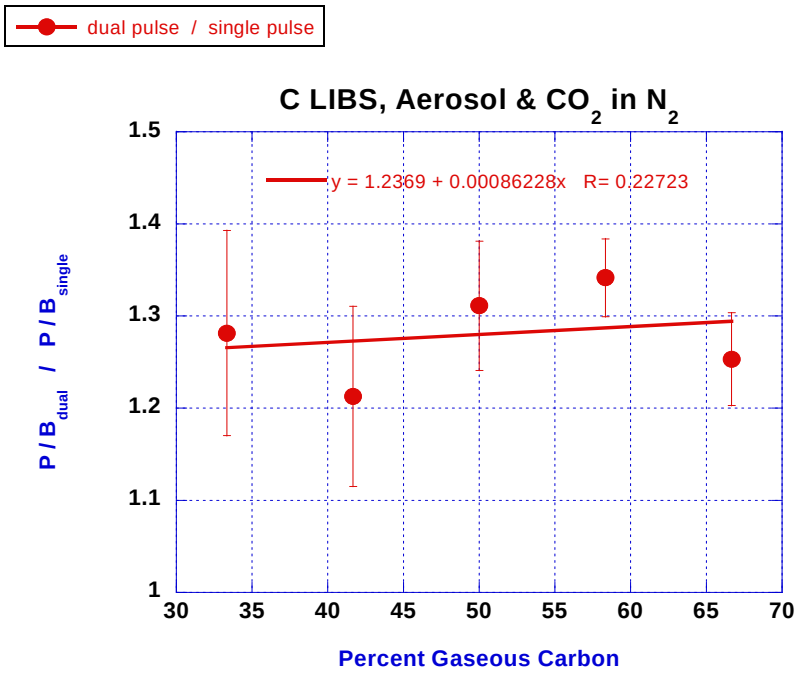

Figure 4.2.18. Ratio of peak-to-base values for the fs-ns configuration to the ns-only configuration. Data in figure was constructed using the data in Figure 4.2.17.

5.0 Summary and Observations

This program explored the feasibility of developing a LIBS based technique for measuring total particulates in a sample containing carbon in gas and particulates species. The program was partly successful in that a LIBS technique was demonstrated for measuring the percentage of gaseous carbon and total particulate carbon in a multi-phase sample. The technique involves establishing a calibration curve that relates the ratio of dual to single-pulse ns-LIBS signals to the percentage of gaseous or total particulate carbon in a multi-phase sample. The program is considered only partly successful because additional research is required to improve the sensitivity so it is a viable technique for other species and for broader ranges of solid and gas ratios.

The program involved research at the University of Florida and at the Air Force Research Laboratory (AFRL). The success of this program was based on the continuation of concepts developed by Prof. Hahn at the University of Florida. In previous research, [Hohreiter and Hahn, 2005] showed that there were significant differences in the LIBS response of carbon contained in solid particles, liquid aerosol particles, and gaseous molecules, with the solid particle response being more pronounced for the same carbon concentration. On this program, Prof. Hahn explored ways of exploiting these differences in sensitivity to determine total particulates in a multi-phase sample. The approach was to investigate the use of single- and dual-pulse ns-LIBS. Calibration curves of LIBS signal, as measured by the peak (P) to base (B) ratio vs. carbon concentration, were obtained for gas and particulate carbon samples. As observed previously, there existed significant differences in the LIBS response of particulate-phase analyte as compared to gaseous-phase analyte. It was also observed that dual-pulse, as compared to single-pulse, ns-LIBS technique provided an enhanced analyte response (as measured by the P/B ratio). These observations were used to formulate a promising technique for measuring total particulates. It was shown

that the ratio of dual- to single-pulse LIBS singles has promise for estimating the percentage of total particulates in a multi-phase sample. However, for this to become a viable technique the sensitivity of the technique needs to be improved.

Literature results suggested that the sensitivity of Professor Hahn's technique might be improved by replacing the ns pre-pulse laser with a fs pre-pulse laser, the idea being that the increased intensity of the fs pre-pulse would more readily ionize the sample. This approach was investigated at the Air Force Research Laboratory (AFRL). An experimental system capable of conducting both ns- and fs-LIBS was constructed at the Propulsion Directorate of AFRL. First, gaseous and solid carbon calibration experiments, similar to those conducted at the University of Florida, were repeated with the AFRL ns-LIBS system. Excellent repeatability of Dr. Hahn's results established that the experimental platform and data processing procedures used by AFRL and the University of Florida were equivalent. Next, measurements, complimentary to and in collaboration with those of Prof. Hahn, were executed using a combination of dual and single-pulse LIBS setups, with a fs pre-pulse being used in the AFRL dual-pulse experiments. In general, the results were similar to those at the University of Florida, in that the fs dual-pulse fs/ns-LIBS P/B ratio was always larger than the corresponding single ns pulse LIBS P/B ratio for gaseous and particulate carbon samples. Unfortunately, for the experimental conditions explored, the *ratio* of the LIBS signal from the fs pre-pulse and the ns main pulse was independent of the percentage of total carbon particulates. The physics associated with this less than expected result is not understood but is believed to be related to the total energy deposited in the plasma generated by the fs pre-pulse and the time duration for depositing the energy. Basically, we speculate that the ns pre-pulse creates a rarefied or low-density plasma with a compression wave that tends to clear the gaseous ions from the region of the plasma responsible for the LIBS signal; whereas, a fs pre-pulse creates a much smaller, high density plasma in which the gaseous species are ionized so quickly that they are not selectively transported to the outer region of the plasma but remain concentrated in the region of the plasma responsible for the LIBS signal.

6.0 Recommendations

The problem of developing an in situ technique for characterizing and studying PM2.5 liquid aerosol and solid particulates in aircraft exhaust type environments is very important because of the impact that PM2.5 have on the environmental as well as on people's health. It is also an extremely difficult measurement problem. Professor Hahn's idea of using the ratio of dual and single pulse LIBS signals to determine the total percentage of particulates in a multi-phase sample is a new, innovative approach that we feel is worth investigating further. However, the ultimate sensitivity of the technique remains a concern. The following recommendations are for research to investigate ways to improve the sensitivity of Professor Hahn's technique. Recommendations are also presented on other approaches for measuring particulates that resulted during the course of this program.

Figure 4.1.6 indicates that the sensitivity of the technique increases as the percentage of gaseous carbon increases; whereas, the technique is weakly dependent on the percentage of gaseous carbon, when the particulate carbon is greater than about 70%. This suggests that for samples with the high particulate loading, the signal is primarily due to carbon from the particulates, a finding consistent with previous research. If this is the case, then either single or dual LIBS could be used to determine the total concentration of carbon with reasonable accuracy because almost all of the analyte signal would come from the particulates. Indeed, the use of dual and signal pulse LIBS may provide a quantitative way of determining when a LIBS signal is basically due to particulates. If this is the case, this would greatly enhance the potential of the single- and dual-pulse ns-LIBS. This point was not fully realized until all of the data were analyzed and summarized; hence resources were not available during the original scope of the work to further investigate the potential. It is therefore recommended that future research on this technique investigate this point.

There are potential ways for increasing the sensitivity of the signal and dual pulse ns-LIBS. It is recommended that additional studies investigate the effect of temporal variations in both the dual-pulse laser-to-laser delay (currently fixed at 1 μs), and the temporal gating of the detector gate (currently fixed at a delay of 8 μs). As more is learned about the temporal nature of analyte dissociation and diffusion within the laser-induced plasma [Diwakar, 2007], additional analyte sensitivity may be realized by further exploiting the differences in solid and gaseous-phase response, and in single and dual-pulse response.

The approach of using a fs pre-pulse to improve the sensitivity of Prof. Hahn's technique did not produce the expected benefits. There is another approach that could be more successful. The idea involves a new method of remote sensing called filament induced breakdown Spectroscopy (FIBS) [Stelmaszczyk, 2004]. When FIBS is used with a LIDR detection technique it can be an effective remote sensing tool that has the potential of providing spatially resolved particulate measurements along a line. It is recommended that FIBS be explored as a way to obtain total percentage of particulates. In particular, the interaction of filaments with aerosol particulates and the resulting analyte response is largely unexplored in the literature. Hence future efforts should include the investigation of using FIBS as the pre-pulse in conjunction with a ns main LIBS pulse at a focal location of the filament.

While conducting this program, several other ideas surfaced as a means of measuring total particulates. In earlier studies, the interaction of lower energy laser pulses with aerosol particles was

noted to yield molecular fragments from the particle that are liberated in the excited electronic state [Omenetto, 2000; Damm, 2001; Dalyander, 2008]. It was also noted that these pulses do not create full laser-induced plasma. In general, this technique is referred to a photofragmentation spectroscopy, and may be considered a complementary technique to LIBS. One advantage of photofragmentation is the ability to pick up volatile organic species and aerosols, notably sulphur-containing species that are historically difficult to detect via LIBS. Future work that combines the photofragmentation and LIBS techniques in a novel multi-pulse sequence could bring additional analytical power to the problem of multi-phase volatile species monitoring.

7.0 Acknowledgements

The authors wish to think Mr. Kyle Frische and Mr Thomas Erickson for the excellent job they did in setting up, checking out, and operating the fs/ns-LIBS system at AFRL. Their help on this project is most appreciated. The authors would also like to think Mr. Michael Asgill for his work at the University of Florida on this project. The authors are most grateful to Ms. Angela Wedding for editing this report and putting it into an acceptable format. The financial support of the U.S. Department of Defense Strategic Environmental Research and Development Program is hereby acknowledged.

8.0 References

Arp, Z. A., Cremers, D. A., Wiens, R. C., Wayne, D. M., Salle, B., and Maurice, S., "Analysis of Water Ice and Water Ice/Soil Mixtures Using Laser-Induced Breakdown Spectroscopy: Application to Mars Polar Exploration," Appl. Spectrosc. 58, pg. 897, 2004.

Baldwin, C., "Particulate Detection in Turbine Exhaust Using Laser-Induced Breakdown Spectroscopy," Proc. of SPIE 6379, 2006.

Blevins, L. G., Shaddix, C. R., Sickafoose, S. M., and Walsh, P. M., "Laser-Induced Breakdown Spectroscopy at High Temperatures in Industrial Boilers and Furnaces," Appl. Opt. 42, pg. 6107, 2003.

Boucher, O., "Air Traffic May Increase Cirrus Cloudiness," Nature 397, pg. 30, 1999.

Braun, A., Korn, G., Liu, X., Du, D., Squier, J., and Mourou, G., "A LIDAR Technique to Measure the Filament Length Generated by a High-Peak Power Femtosecond Laser Pulse in Air," Opt. Lett. 20, pg. 73, 1995.

Calibration," TSI Quarterly, 4(2): 3-8.

Chin, S. L., et al. "The Propagation of Powerful Femtosecond Laser Pulsed in Optical Media: Physics, Applications, and New Challenges'', Can. J. Phys. 83: 863-905, 2005.

Dalyander, P.S., D.W. Hahn. *Applied Spectroscopy*, 62:1028-1037 (2008).

Damm, C. J.,D. Lucas, R.F. Sawyer, and C.P. Koshland, Appl. Spectrosc. **55**, 1478 (2001).

Diwakar, P.K., P.B. Jackson, D.W. Hahn, Investigation of Multi-component Aerosol Particles and the Effect on Quantitative Laser-induced Breakdown Spectroscopy: Consideration of Localized Matrix Effects, *Spectrochimica Acta Part B*, 62:1466-1474 (2007).

Gibbon, Paul, Short Pulse Laser Interaction with Matter: An Introduction, Imperial College Press (2005).

Gunaratne, T., Kangas, M., Singh, S., Gross, A., and Dantus, M., "Influence of Bandwidth and Phase Shaping on Laser Induced Breakdown Spectroscopy with Ultrashort Laser Pulses," Chem. Phys. Lett. 423, pg. 197, 2006.

Hahn, D. W., et al., "Discrete Particle Detection and Metal Emissions Monitoring Using Laser-Induced Breakdown Spectrocopy," Appl. Spectrosc. 51: 1836-1844, 1997.

Hahn, D. W., "Laser-Induced Breakdown Spectroscopy for Sizing and Elemental Analysis of Discrete Aerosol Particles," Appl. Phus. Letters, 72L2960-2962, 1998.

Hahn, D. W. and Lunden, M. M., "Detection and Analysis of Aerosol Particles by Laser-Induced Breakdown Spectroscopy," Aerosol Sci. Technol. 33, pg. 30, 2000.

Hahn et al. Aerosol generation system, Rev. Sci. Instrum. 72(9) 3706, 2005.

Hidalgo, M., Núñez, P. Cavalli, G. Petrucci, and N. Omenetto, Appl. Spectrosc. **54**, 1805 (2000).

Hohreiter V., and D.W. Hahn. Calibration effects for laser-induced breakdown spectroscopy of gaseous sample streams: Analyte response of gaseous phase species vs. solid phase species, *Analytical Chemistry*, 77:1118-1124 (2005).

Itoh, S., Shinoda, M., Kitagawa, K., Arai, N., Lee, Y-I., Zhao, D., and Yamashita, H., "Spatially Resolved Elemental Analysis of a Hydrogen-Air Diffusion Flame by Laser-Induced Plasma Spectroscopy (LPIS)," Microchemical Journal 70, pg. 143, 2001.

Iwasaki, A., Akozbek, N., Ferland, B., Luo, Q., Roy, G., Bowden, C. M., and Chin, S. L., "A LIDAR Technique to Measure the Filament Length Generated by a High-Peak Power Femtosecond Laser Pulse in Air," Appl. Phys. B 76, pg. 231, 2003

Jin, Z., Zhang, J., Xu, M. H., Lu, X., Li, Y. T., Wang, Z. H., Wei, Z. Y., Yuan, X. H., and Yu, W., "Control of Filamentation Induced by Femtosecond Laser Pulses Propagating in Air," Opt. Express 13, pg. 10424, 2005.

Karcher, B., Yu, F., Schroder, F. P., and Turco, R. P., "Ultrafine Aerosol Particles in Aircraft Plumes: Analysis of Growth Mechanisms," Geophys. Res. Lett. 25, pg. 2793 (1998).

Karcher, B., Busen, R., Petzold, A., Schroder, F. P., and Schumann, U., "Physiochemistry of Aircraft-Generated Liquid Aerosols, Soot, and Ice Particles 2. Comparison with Observation and Sensitivity Studies," J. Geophys. Res. 103, pg. 17129, 1998-b.

Kasparian, J et al, "White Light Filaments for Atmospheric Analysis," Science 301, pg. 61, 2003.

Le Drogoff, B., Margot, J., Chaker, M., Sabsabi, M., Barthelemy, O., Johnston, T. W., Laville, S., Vidal, F., and von Kaenel, Y., "Temporal Characterization of Femtosecond Laser Pulses Induced Plasma for Spectrochemical Analysis of Aluminum Alloys," Specrochem. Acta B 56, pg. 987, 2001.

Lee, W-B., Wu, J., Lee, Y-I., and Sneddon, J., "Recent Applications of Laser-Induced Breakdown Spectrometry: A Review of Material Approaches," Appl. Spectrosc. Rev. 39, pg. 27, 2004.

Margetic, V., Pakulev, A., Stockhaus, A., Bolshov, M., Niemax, K., and Hergenroder, R., "A Comparison of Nanosecond and Femtosecond Laser-Induced Plasma Spectroscopy of Brass Samples," Specrochem. Acta B 55, pg. 1771, 2000.

Nunez, M. H., Cavalli, P., Petrucci, G., and Omenetto, N., "Analysis of Sulfuric Acid Aerosols by Laser-Induced Breakdown Spectroscopy and Laser-Induced Photofragmentation," Appl. Spectrosc. 54, pg. 1805, 2000.

Penner, J. E., Lister, D. H., Griggs, D. J., and Dokken, D. J. eds., "Aviation and the Global Atmosphere," Intergovernmental Panel on Climate Control, www.grida.no/climate/ipcc/aviation/index.htm, 1999.

Petzold, A. and Schroder, F. P., "Jet Engine Exhaust Aerosol Characterization," Aerosol Sci. Technol. 28, pg. 62 (1998)

Putaud, J-P., *et al*, "A European Aerosol Phenomenology—2: Chemical Characteristics of Particulate Matter at Kerbside, Urban, Rural and Background Sites in Europe," Atmospheric Environment 38. pg. 2579 (2004).

Radzlemski, L. J., et al, "Time-Resolved Laser-Induced Breakdown Spectrometry of Aerosol," Anal. Chem. 55, 1246-1252, 1983.

Rogers, D. C., DeMott, P. J., Kreidenweis, S. M., and Chen, Y., "Measurements of Ice Nucleating Aerosols During SUCCESS," Geophys. Res. Lett. 25, pg. 1383 (1998).

Schafer, K., et al., "Nonintrusive Optical Measurements of Aircraft Engine Exhaust Emissions and Comparison with Standard Intrusive Techniques," Appl. Opt. 39, pg. 441, 2000.

Schumann, U., Arnold, F., Busen, R., Curtiss, J., Karcher, B., Kiendler, A., Petzold, A., Schlager, H., Schroder, F., and Wohlrom, K. H., "Influence of Fuel Sulfur on the Composition of Aircraft Exhaust Plumes: The Experiments SULFUR 1-7," J. Geophys. Res. 107, pg. 4247, 2002.

Sirven, J. B., Bousquet, B., Canioni, L., and Sarger, L., "Time-Resolved and Time-Integrated Single-Shot Laser-Induced Plasma Experiments Using Nanosecond and Femtosecond Laser Pulses," Specrochem. Acta B 59, pg. 1033, 2004.

Song, K., Lee, Y-I., and Sneddon, J., "Applications of Laser-Induced Breakdown Spectrometry," Appl. Spectrosc. Rev. 32, pg. 183, 1997.

Stelmaszezyk, K., Rohwetter, P., and et al. "Long-distance Remote Laser-Induced Breakdown Spectroscopy Using Filamentation in Air", Appl. Phys. Lett., 85, 18, 3977-3979, 1 Nov. 2004.

Twohy, C. H. and Gandrud, B. W., "Electron Microscope Analysis of Residual Particles from Aircraft Contrails," Geophys. Res. Lett. 25, pg. 1359 (1998).

Wilson, C. W., Petzold, A., Nyecki, S., Schumann, U., and Zellner, R., "Measurement and Prediction of Emissions of Aerosols and Gaseous Precursors from Gas Turbine Engines (PartEmis): an Overview," Aerospace Sci. Technol. 8, pg. 131, 2004.

Windom, B.C., P.K. Diwakar, D.W. Hahn. Dual-Pulse LIBS for Analysis of Gaseous and Aerosol Systems: Plasma-Analyte Interactions, *Spectrochimica Acta Part B*, 61:788-796 (2006).

Zeldovich and Raizer, Vol.1. Physics of Shock Waves and High-Temperature Hydrodynamic Phenomena (AP,1966).